

8-2012

# Photochemical Oxidation Studies of Porphyrin Ruthenium Complexes

Eric Vanover

Western Kentucky University, [eric.vanover@topper.wku.edu](mailto:eric.vanover@topper.wku.edu)

Follow this and additional works at: <http://digitalcommons.wku.edu/theses>

 Part of the [Organic Chemistry Commons](#)

---

## Recommended Citation

Vanover, Eric, "Photochemical Oxidation Studies of Porphyrin Ruthenium Complexes" (2012). *Masters Theses & Specialist Projects*. Paper 1201.  
<http://digitalcommons.wku.edu/theses/1201>

This Thesis is brought to you for free and open access by TopSCHOLAR®. It has been accepted for inclusion in Masters Theses & Specialist Projects by an authorized administrator of TopSCHOLAR®. For more information, please contact [topscholar@wku.edu](mailto:topscholar@wku.edu).



PHOTOCHEMICAL OXIDATION STUDIES OF PORPHYRIN RUTHENIUM  
COMPLEXES

A Thesis  
Presented to  
The Faculty of the Department of Chemistry  
Western Kentucky University  
Bowling Green, Kentucky

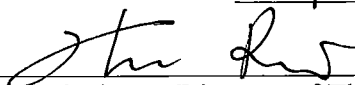
In Partial Fulfillment  
Of the Requirements for the Degree  
Master of Science

By  
Eric Vanover

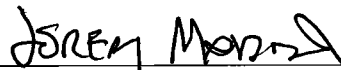
August 2012

PHOTOCHEMICAL OXIDATION STUDIES OF PORPHYRIN RUTHENIUM  
COMPLEXES

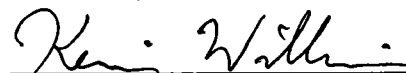
Date Recommended 07-23-12



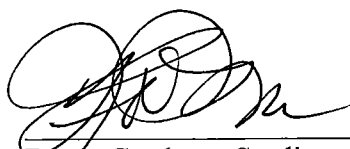
Dr. Rui Zhang, Director of Thesis



Dr. Jeremy Maddox



Dr. Kevin Williams



Dean, Graduate Studies and Research

8/23/12

Date

## ACKNOWLEDGEMENTS

It is my pleasure to sincerely thank all the outstanding people who were an active part of my research and made this thesis possible. First of all, I would like to express my deepest gratitude to my research advisor Dr. Rui Zhang for his guidance, patience, advice, encouragement, understanding and moral support throughout my study at Western Kentucky University. In particular, his perpetual kindness and devoted attitude guided me through any trouble. My thesis would not have been possible without his selfless support and ingenuity.

During the course of my study and compilation of the thesis, my sincere thanks go to the following professors and members of my research group who I have worked with and learned from. I am forever grateful to have Dr. Kevin Williams and Dr. Jeremy Maddox to serve on my thesis committee. Their many suggestions, advice and discussions were very helpful. My sincere thanks also go to Dr. Eric Conte for his help in GC technique support.

I wish to thank all my research group members: Chris Abebrese, Yan Huang, Helen Thompson, Alice Pan, and Zihbo Yuan for their support and assistance during my research. They are all specially acknowledged for giving me enjoyable and memorable friendship.

## TABLE OF CONTENTS

Chapter	Page
1. Introduction.....	1
1.1 General.....	1
1.2 Biomimetics of Cytochrome P-450Enzymes.....	8
1.3 High Valent Metal-Oxo Species.....	10
1.4 Photocatalytic Aerobic Oxidations.....	12
2. Experimental Section .....	15
2.1 Materials & Chemicals .....	15
2.2 Photocatalytic Oxidation Studies.....	15
2.3 Kinetic Isotope Effect (KIE) Study.....	16
2.4 Physical Measurements .....	17
2.5 Reagents Purification.....	17
3. Photocatalytic Aerobic Oxidation by a Bis-Porphyrin- Ruthenium(IV) $\mu$ -Oxo Dimer	
3.1 Introduction.....	18
3.2. Synthesis and Spectroscopic Characterization of <i>meso</i> -Tetraphenylporphyrin H <sub>2</sub> Por ( <b>1a-c</b> ).....	20
3.3.1. Synthesis and Characterization of Carbonyl Ruthenium(II) Porphyrin Complexes ( <b>2</b> ).....	23
3.3.2. Preparation of Carbonyl (5,10,15,20-terraphenylporphyrinato) Ruthenium(II) [Ru <sup>II</sup> (CO)TPP] ( <b>2a</b> ).....	24

3.3.3 Preparation of Carbonyl (5,10,15,20-tetrakis (pentafluorophenyl)porphyrinato) Ruthenium(II) [Ru <sup>II</sup> (CO)TPFPP] ( <b>2d</b> ).....	27
3.4.1 Synthesis and Characterization of Bis-Porphyrin-Ruthenium(IV) $\mu$ -Oxo Dimers ( <b>3</b> ).....	29
3.4.2 Photocatalytic Aerobic Oxidation by a Bis-Porphyrin- Ruthenium(IV) $\mu$ - Oxo Dimer ( <b>3</b> ).....	32
3.4.3 Photocatalytic Aerobic Oxidation by a Bis-Porphyrin-Ruthenium(IV) $\mu$ -Oxo Dimer ( <b>3c</b> ).....	35
4. A Novel Photochemical Generation of <i>trans</i> -Dioxoruthenium(IV) Porphyrin	
4.1 Introduction.....	38
4.2. Preparation of dichlororuthenium(IV) porphyrin [Ru <sup>IV</sup> (Por)Cl <sub>2</sub> ] .....	43
4.3. Preparation of porphyrin- ruthenium(IV) dichlorates [Ru <sup>IV</sup> (Por)(ClO <sub>3</sub> ) <sub>2</sub> ] .	45
4.4. Photolysis of porphyrin–ruthenium(IV) dichlorates [Ru <sup>IV</sup> (Por)(ClO <sub>3</sub> ) <sub>2</sub> ]...	46
4.4.1 Photolysis of porphyrin–ruthenium(IV) dibromates [Ru <sup>IV</sup> (Por)(BrO <sub>3</sub> ) <sub>2</sub> ].	48
4.5. Generation Procedure for Photosynthesis of <i>trans</i> -Dioxoruthenium(VI) Porphyrins [Ru <sup>VI</sup> (Por)(O) <sub>2</sub> ] <b>6</b> .....	49
5. Conclusions.....	51
References.....	52
Publications and Presentations.....	62
Abbreviations and Symbols.....	65

## LIST OF FIGURES

<u>Figure</u>	<u>Page</u>
1. Structure of iron protoporphyrin IX (Heme <i>b</i> ).....	3
2. X-ray structure of cytochrome P450 <sub>cam</sub> .....	5
3. UV-Vis spectroscopy of H <sub>2</sub> TPP ( <b>1a</b> ) CH <sub>2</sub> Cl <sub>2</sub> .....	22
4. <sup>1</sup> H-NMR spectroscopy of H <sub>2</sub> TPP <b>1a</b> in CDCl <sub>3</sub> .....	22
5. UV-Vis of [Ru <sup>II</sup> (CO)TPP] in CH <sub>2</sub> Cl <sub>2</sub> ( <b>2a</b> ).....	26
6. <sup>1</sup> H-NMR of [Ru <sup>II</sup> (CO)TPP] ( <b>2a</b> ).....	26
7. UV-Vis of [Ru <sup>II</sup> (CO)TPFPP] ( <b>2d</b> ) in CHCl <sub>3</sub> .....	28
8. of [Ru <sup>II</sup> (CO)TPFPP] ( <b>2d</b> ) in CDCl <sub>3</sub> .....	28
9. UV-Vis of [Ru <sup>IV</sup> (TPP)] <sub>2</sub> O in CHCl <sub>3</sub> ( <b>3a</b> ).....	31
10. <sup>1</sup> H-NMR of [Ru <sup>IV</sup> (TPP)] <sub>2</sub> O ( <b>3a</b> ) in CDCl <sub>3</sub> .....	31
11. UV-vis spectral change of <b>1a</b> (6×10 <sup>-6</sup> M) in the presence of excess Ph <sub>3</sub> P (50 mM) upon irradiation with a 300-W visible lamp (λ <sub>max</sub> 420 nm) in anaerobic CH <sub>3</sub> CN solution. ....	32
12. (A) Typical UV-Vis spectra of Ru <sup>IV</sup> (TPP)Cl <sub>2</sub> , <b>4a</b> , (dashed) and Ru <sup>IV</sup> (TPP)(ClO <sub>3</sub> ) <sub>2</sub> , <b>5a</b> , (solid) in CH <sub>3</sub> CN. (B) <sup>1</sup> H NMR spectrum of Ru <sup>IV</sup> (TPP)Cl <sub>2</sub> , <b>4a</b> , (top) and Ru <sup>IV</sup> (TPP)(ClO <sub>3</sub> ) <sub>2</sub> , <b>5a</b> , (bottom) in CDCl <sub>3</sub> .....	45
13. Examples of generation of <i>trans</i> -dioxoruthenium(VI) species ( <b>6</b> ) by photolysis of the corresponding dichlorate precursors ( <b>5</b> ). ....	47
14. UV–Vis spectral change of <b>1a</b> (8 x10 <sup>-6</sup> M) with 5-fold excess of AgBrO <sub>3</sub> in anaerobic CH <sub>3</sub> CN solution upon irradiation with a 100W tungsten lamp at 22°C over 80 min.....	49



## LIST OF TABLES

<u>Table</u>	<u>Page</u>
<b>Table 1.</b> Aerobic Photocatalytic Oxidation of <i>cis</i> -cyclooctene with Diruthenium(IV) $\mu$ -Oxo Porphyrins.....	34
<b>Table 2.</b> Turnover Numbers for Alkenes and Benzylic C-H Oxidations Using [Ru <sup>IV</sup> (4-CF <sub>3</sub> -TPP)(OH)] <sub>2</sub> O ( <b>3c</b> ) as the Photocatalyst.....	36

## LIST OF SCHEMES

<u>Scheme</u>	<u>Page</u>
1. Monooxygenase reaction.....	4
2. Stereospecific hydroxylation of the exo C-H bond at position 5 of camphor by cytochrome P450 <sub>cam</sub> .....	5
3. Typical metalloporphyrin-mediated reactions.....	7
4. Hydroxylation of hydrocarbons with 2,6-dichloropyridine <i>N</i> -oxide catalyzed by Ru <sup>II</sup> (CO)TPFPP.....	10
5. “Pacman” diiron(III)- $\mu$ -oxo-bisporphyrin complex.....	14
6. Photocatalytic aerobic oxidation by a bis-porphyrin-ruthenium(IV) $\mu$ -oxo dimer.....	19
7. Synthesis of porphyrin systems (1).....	21
8. Synthesis of [Ru <sup>II</sup> (CO)Por] (2).....	24
9. Synthesis of [Ru <sup>II</sup> (CO)TPFPP] (2d).....	27
10. Synthesis of [Ru <sup>IV</sup> (Por)(OH)] <sub>2</sub> O (3).....	30
11. Generation of high-valent metal-oxo species by photo-induced ligand cleavage reactions.....	41
12. Photochemical generation of <i>trans</i> -dioxoruthenium(VI) porphyrins.....	42
13. Synthesis of dichlororuthenium(IV) porphyrins complexes 4.....	44

# PHOTOCHEMICAL OXIDATION STUDIES OF PORPHYRIN RUTHENIUM COMPLEXES

Eric Vanover

August 2012

66 Pages

Directed by: Dr. Rui Zhang, Dr. Jeremy Maddox, and Dr. Kevin Williams

Department of Chemistry

Western Kentucky University

In nature, transition metal containing enzymes display many biologically important, attractive and efficient catalytic oxidation reactions. Many transition metal catalysts have been designed to mimic the predominant oxidation catalysts in nature, namely, the cytochrome P450 enzymes. Ruthenium porphyrin complexes have been the center of this research and have successfully been utilized, as catalysts, in major oxidation reactions, such as the hydroxylation of alkanes. The present work focuses on photocatalytic studies of aerobic oxidation reactions with well characterized ruthenium porphyrin complexes.

The photocatalytic studies of aerobic oxidation reactions of hydrocarbons catalyzed by a bis-porphyrin-ruthenium(IV)  $\mu$ -oxo dimer using atmospheric oxygen as the oxygen source in the absence of co-reductants were investigated. The ruthenium(IV)  $\mu$ -oxo bisporphyrin (**3a-d**) was found to catalyze aerobic oxidation of a variety of organic substrates efficiently. By comparison, **3d** was found to be a more efficient photocatalyst than the well-known **3a** under identical conditions. A KIE at 298K was found to be larger than those observed in autoxidation processes, suggesting a nonradical mechanism that involved the intermediacy of ruthenium(V)-oxo species as postulated. The reactivity order in the series of ruthenium(IV)  $\mu$ -oxo bisporphyrin complexes follows TPFPP>4-CF<sub>3</sub>TPP>TPP, and is consistent with expectations based on the electrophilic nature of the ruthenium(IV)  $\mu$ -oxo bisporphyrin species.

The *trans*-dioxoruthenium(VI) porphyrins have been among the best characterized metal-oxo intermediates and their involvement as the active oxidant in the hydrocarbon oxidation have been extensively studied. In addition to the well-known chemical methods, we developed a novel approach for generation of *trans*-dioxoruthenium(VI) porphyrins with visible light by extension of the known photo-induced ligand cleavage reactions. A series of *trans*-dioxoruthenium(VI) porphyrin complexes (**6a-d**) were photochemically synthesized and spectroscopically characterized by UV-vis, and <sup>1</sup>H-NMR.

## I. INTRODUCTION

### 1.1. General

Catalytic oxidations are core transformations in organic synthesis. Millions of tons of oxygenated compounds are annually produced and applied worldwide, ranging from pharmaceutical to large-scale commodities.<sup>1</sup> Many stoichiometric oxidants with heavy metals are expensive and/or toxic and, thus, impractical. The ideal green catalytic oxidation process would use molecular oxygen or hydrogen peroxide as the primary oxygen source, recyclable catalysts in nontoxic solvents, and an inexpensive energy source.<sup>2</sup> The development of new processes that employ transition metals as substrate-selective catalysts and a stoichiometric, environmentally friendly oxygen source, such as molecular oxygen or hydrogen peroxide, is one of the most significant goals in oxidation chemistry.<sup>3</sup> These oxidants are atom efficient and produce water as the only by-product, and are becoming more important in fine chemical manufacturing.<sup>4</sup>

In biological systems, catalytic oxidations facilitated by oxidative enzymes are fundamental in many biosynthesis and biodegradation processes.<sup>5</sup> Hayaishi and co-workers revealed that evolution has found many ways to utilize atmospheric dioxygen to functionalize molecules through the use of a diverse set of cofactors.<sup>6</sup> Flavin, non-heme iron, copper, and metalloporphyrin complexes have all been employed to utilize atmospheric dioxygen in an oxygenase catalytic cycle, resulting in the incorporation of one or both oxygen atoms into the substrate.<sup>6</sup> Most of these biological oxidations are mediated by heme-containing oxygenases. Possibly the most intriguing enzyme belonging to this array of oxygenases is the ubiquitous cytochrome P-450 monooxygenase. In nature the CYP450 enzymes have exhibited a vast range of oxidation

reactions, which include important transformations, such as alkene epoxidation and alkane hydroxylation, and many of which are characterized by high degrees of chemo-, regio-, and enantioselectivities.<sup>5-7</sup> Cytochrome P450 has launched many research efforts, including this work. Although there are a great many biological enzymes, the CYP450s command a variety of crucial roles in living creatures.

Many members of the cytochrome P450 superfamily of hemoproteins are currently known, and the numbers continue to grow as more genomes are sequenced. To date, over 8100 distinct cytochrome P450 genomes are known to exist, but few have been studied in detail. The cytochrome P450s have been found in every facet of life inhabiting earth, including plants, bacteria, fungi, insects, human beings and so on. Moreover, they can be isolated in numerous mammalian tissues as well, like liver, kidney, lung, and intestine.<sup>6</sup> If one had to briefly highlight the duties of these oxygenases, two main functions would be discussed. One is metabolism of drugs and xenobiotics (compounds exogenous to the organism) as a detoxification role via degradation and oxidation, which increases water solubility necessary for excretion. A second broad functional role is in the biosynthesis of critical signaling molecules used for control of development and homeostasis. In mammalian tissues the P450s play these roles through the metabolism of drugs and xenobiotics, the synthesis of steroid hormones and fat-soluble vitamin metabolism, and the conversion of polyunsaturated fatty acids to biologically active molecules, respectively.<sup>6</sup>

The consequential metabolic role coupled with the unique chemistry and physical properties of the cytochrome P450s proves to be irresistible for scientists in many disciplines. Relevance to human health is the focus of pharmacologists and toxicologists.

The role of metal centers and their associated unique spectral properties in the cytochrome P450s is a magnet for bioinorganic chemists and biophysicists.<sup>8</sup> The difficult conversion of unactivated hydrocarbons attracted the bioorganic chemist.<sup>8</sup> A perpetual challenge is to understand how the diverse set of substrate specificities and metabolic transformations are determined by the precise nature of the heme-iron oxygen and protein structure. Solving the intricacies of the “active oxygen” intermediates, which serve as efficient catalysts, remains an area of fervent research.<sup>4</sup> The most common heme prosthetic group found in heme-containing enzymes is the iron protoporphyrin IX (heme *b*) complex,<sup>8</sup> which is reported as the active site of the heme enzymes (Figure 1).<sup>8</sup>

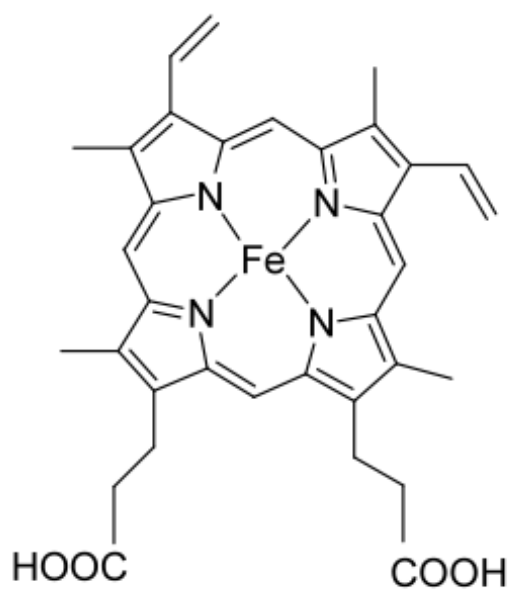
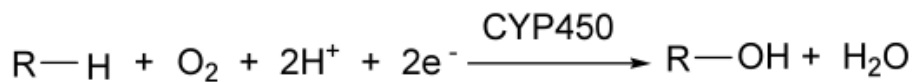


**Figure 1.** Structure of iron protoporphyrin IX (Heme *b*)

Cytochrome P-450 enzymes are classified further as monooxygenases Scheme 1. Therefore, they incorporate one oxygen atom from atmospheric molecular oxygen into a given substrate and reduce the second oxygen to water, utilizing reducing agents, such as NADH (nicotinamide adenine dinucleotide) or NADPH (nicotinamide adenine

dinucleotide phosphate), as electron donor via electron transport protein systems.<sup>8</sup>



**Scheme 1.** Monooxygenase reaction.

The reduced protein efficiently binds carbon monoxide with a strong absorption band (the Soret band) at 450 nm, giving rise to its name. The majority of the CYP450 enzymes are membrane-bound, usually relegated to the inner mitochondrial and the endoplasmic reticulum of microsomal membranes.<sup>8</sup> The majority of physiological substrates, such as steroids and fatty acids as well as xenobiotic molecules, are highly hydrophobic. A soluble, camphor-inducible, bacterial P450 monooxygenase (P450 CAM) system was discovered in *Pseudomonas putida* by Gunsalus and coworkers.<sup>8,9</sup> Being soluble, it was quickly possible to purify this P450 enzyme in large quantity. The enigma of cytochrome P450s structure was deciphered when Poulos et al. provided the first three-dimensional structure of the cytochrome P450cam (Figure 2) in 1986, which catalyzes the stereospecific hydroxylation of the exo C<sub>5</sub>-H bond of camphor (Scheme 2 ).<sup>10</sup>



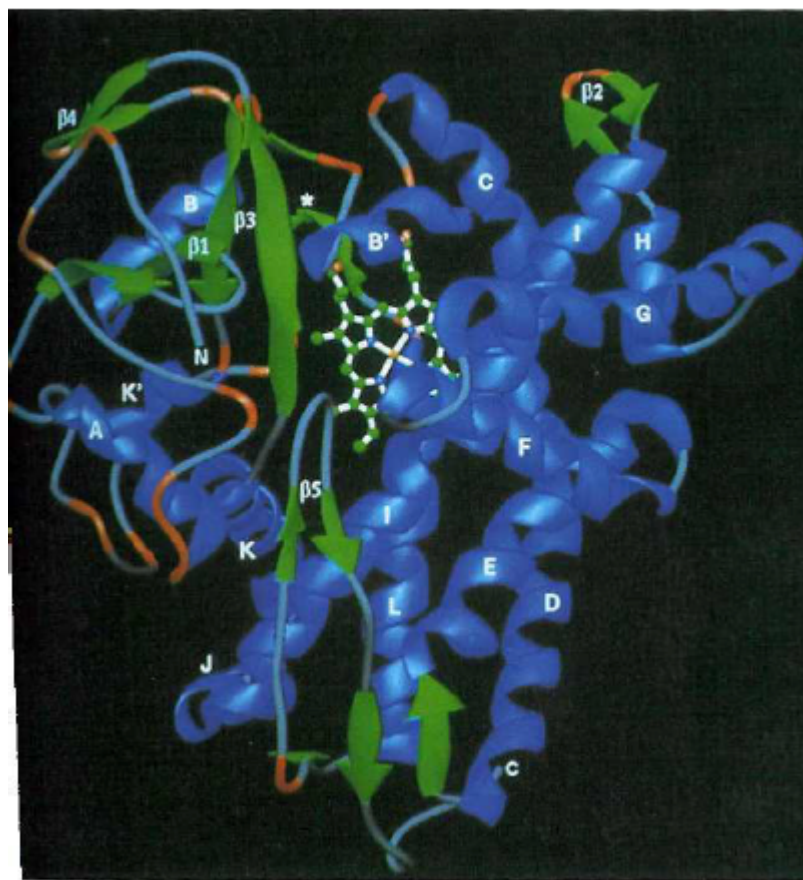
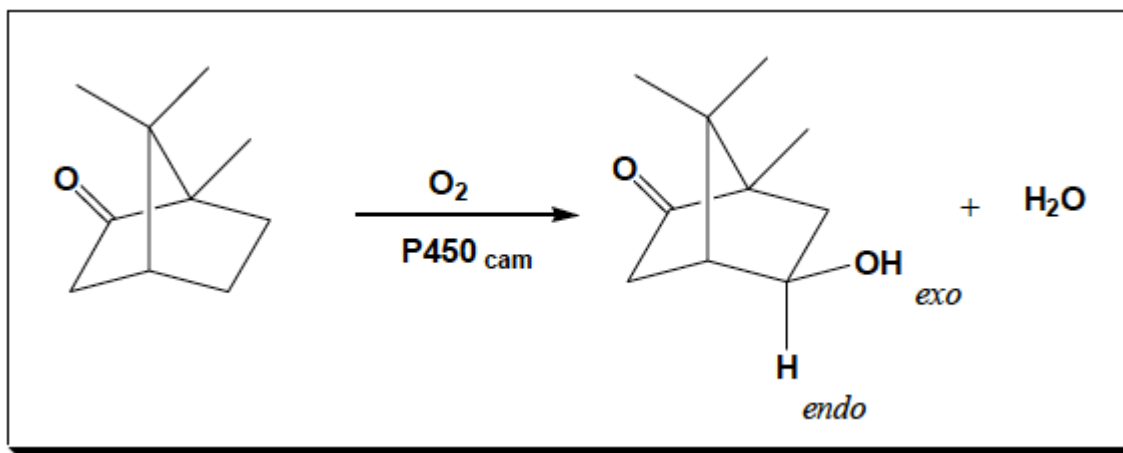
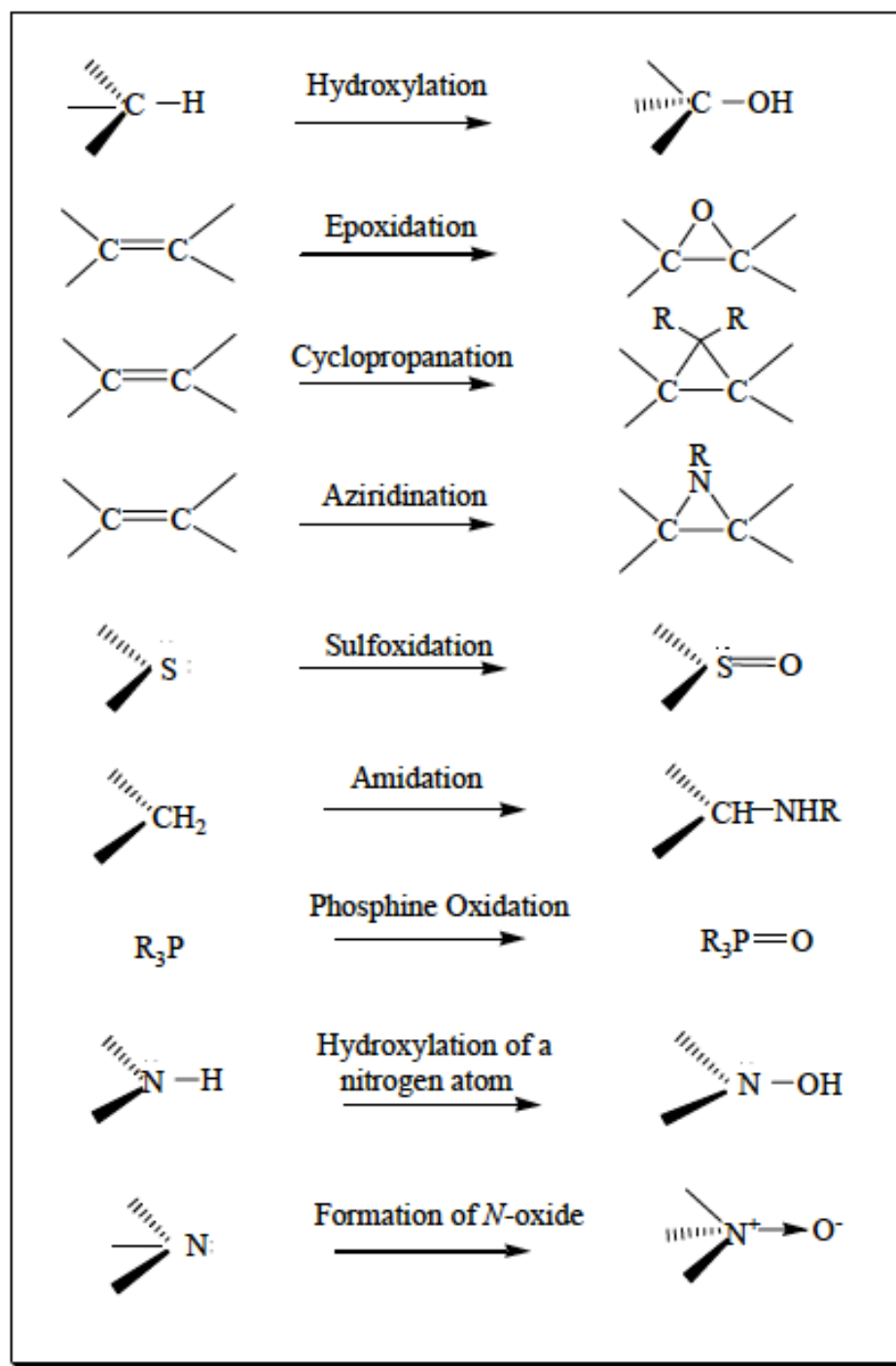


**Figure 2.** X-ray structure of cytochrome P450<sub>cam</sub>



**Scheme 2.** Stereospecific hydroxylation of the *exo* C-H bond at position 5 of camphor by cytochrome P450<sub>cam</sub>

More than 50 years after the discovery of cytochrome P450 enzymes, the true oxidative species (the putative high-valent iron-oxo intermediate) is still indefinative.<sup>10</sup> The oxidant in a P450 enzyme is usually thought to be an iron(IV)-oxo porphyrin radical cation, termed Compound I, by analogy to the intermediates formed in peroxidase and catalase enzymes.<sup>11</sup> The development of new systems utilizing iron, manganese, and ruthenium transition metals have been employed as substrate-selective catalysts of biomimic models of the cytochrome P450 enzymes.<sup>10</sup> In the past decades, many synthetic metalloporphyrin complexes have been reported as model compounds of heme-containing enzymes and catalysts for a variety of selective oxidation reactions (Scheme 3).<sup>10</sup> This work was driven by the desire for the better understanding of the intricate mechanisms of biochemical oxidations using simple biomimetic models.



**Scheme 3.** Typical metalloporphyrin-mediated oxidation reactions

## 1.2. Biomimetic Models of Cytochrome P450 Enzymes

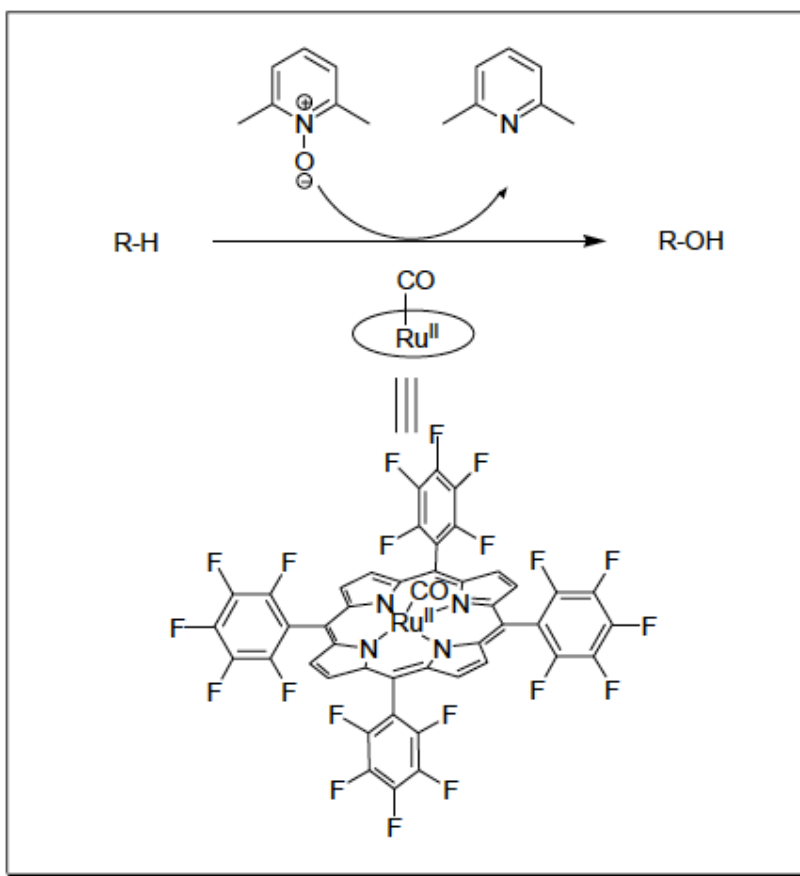
The selective oxygenation of alkanes and alkenes is one of the most important technologies for the conversion of petroleum derivatives to valuable commodity chemicals.<sup>12</sup> Current technologies have seen scrutiny, citing their environmentally unfriendly nature. The development of more efficient alternatives using dioxygen ( $O_2$ ), hydrogen peroxide or other abundant and environmentally friendly oxidants is of the utmost importance.<sup>13,14</sup> However, the high kinetic barrier of the  $O_2$  triplet state impedes direct oxidation by molecular oxygen or hydrogen peroxide. Transition metals may hold the key, if in the appropriate oxidation state. Such complexes can form dioxygen adducts with triplet  $O_2$ , and, thus, are capable of undergoing monooxygenase reactions with organic substrates.<sup>8</sup>

To mediate intrinsically difficult oxidations with molecular oxygen, nature chose iron porphyrins nestled at the heme center of cytochrome P450 monooxygenases.<sup>15</sup> Accordingly, substantial efforts have been directed to the synthesis of biomimetic transition metal catalysts for stereo- and regioselective organic oxidations.<sup>16</sup> Metalloporphyrin catalysts utilizing iron, manganese and ruthenium have received keen attention, promising effective catalytic systems for hydrocarbon oxidation. The past decades have witnessed the development of various cytochrome P450 models, and their subsequent application to hydrocarbon oxidations with the aims of both developing useful catalysts and probing the mechanisms of these processes.<sup>10</sup>

Groves et al, first reported an iron porphyrin system as a CYP450 model that demonstrated effective catalysis of stereospecific alkene epoxidation and alkane hydroxylation in 1979.<sup>17</sup> The use of iodosylbenzene as an oxygen transfer agent, in the

model system, sought to mimic the chemistry of CYP450. The active oxidant intermediate, although not detected under turnover conditions, was thought to be an iron(IV)-oxo porphyrin radical cation, which is also known as compound I species, an intermediate in peroxidase and catalase enzymes. In 2007 works reported by Collins and co-workers displaced the standing assumption that compound I species were the intermediates. Iron(V)-oxo species have been proposed as key reactive intermediates in the catalysis of oxygen-activating enzymes and synthetic catalysts.<sup>18</sup>

Ruthenium porphyrin complexes are among the most extensively studied biomimetic catalysts for hydrocarbon oxidation because of their periodic relationship to the biologically significant iron. A prime example, ruthenium(II) tetrakis(pentafluorophenyl)porphyrin [ $\text{Ru}^{\text{II}}(\text{CO})\text{TPFP}$ ] efficiently catalyzed the hydroxylation of unactivated alkanes, the cleavage of ethers, and the oxygenation of benzene with 2,6-dichloropyridine *N*-oxide as the oxidant under mild, nonacidic conditions (Scheme 4).<sup>15</sup>



**Scheme 4.** Hydroxylation of hydrocarbons with 2,6-dichloropyridine *N*-oxide catalyzed by  $\text{Ru}^{\text{II}}(\text{CO})\text{TPFPF}$

### 1.3. High-Valent Transition Metal-Oxo Species

High-valent oxo metalloporphyrins have been known as reactive intermediates in the catalytic cycles of many heme enzymes and in the oxidation reactions mediated by synthetic metalloporphyrins.<sup>10,12</sup> Studies using synthetic metalloporphyrins as models for cytochrome P450 have afforded important insights into the nature of the enzymatic processes.<sup>10,19</sup> In the past decade, there have been many reports on the chemistry of iron(IV) porphyrins; however, the intrinsic reactivity and liability of high-valent iron-oxo complexes hamper detailed mechanistic studies on their oxidation chemistry.<sup>20</sup> In view of this, there has been growing interest in substituting iron with other metals,<sup>20</sup> such as

manganese and ruthenium.

The chemistry of high-valent manganese-oxo intermediates has received considerable attention.<sup>21</sup> Manganese porphyrins have been shown to have unusually high reactivity toward olefin epoxidation and alkane hydroxylation.<sup>21</sup> For instance, the reaction of the water-soluble tetra-*N* methyl-4-pyridylporphyrinatomanganese(III) [Mn<sup>III</sup>(TMPyP)] with a variety of oxidants was first reported by Meunier and co-workers to produce a manganese-oxo intermediate that underwent rapid oxo-aqua interconversion.<sup>21</sup> Recently, the detection of an oxomanganese(V) porphyrin intermediate under ambient conditions by using rapid mixing stopped-flow techniques has allowed a direct assessment of its reactivity.<sup>22</sup>

Ruthenium porphyrin complexes are among the most extensively studied biomimetic catalysts for hydrocarbon oxidation because of the rich coordination and redox chemistry of ruthenium. Ruthenium boasts the greatest range oxidation states from -2 to +8 in various ligand environments. Since ruthenium complexes have a variety of useful characteristics, including high Lewis acidity, high electron transfer ability, low redox potentials and stability of reactive metal species, a great number of new and significant reactions have been developed by using both stoichiometric and catalytic amounts of ruthenium complexes.<sup>5</sup>

In particular, *trans*-dioxoruthenium(VI) porphyrin complexes are a significant class of ruthenium oxidants, that are neutral and readily dissolve in nonpolar organic solvent, and yet are reactive toward alkene epoxidations and alkane hydroxylations. Furthermore, they also can be modified by attaching chiral auxiliaries onto the porphyrinato ligands providing an access to highly reactive chiral metal-oxo reagents.<sup>5</sup> In

this work, a new photochemical method has been developed to produce *trans*-dioxoruthenium(VI) complexes that possess porphyrin ligands of various electronic nature.<sup>23</sup>

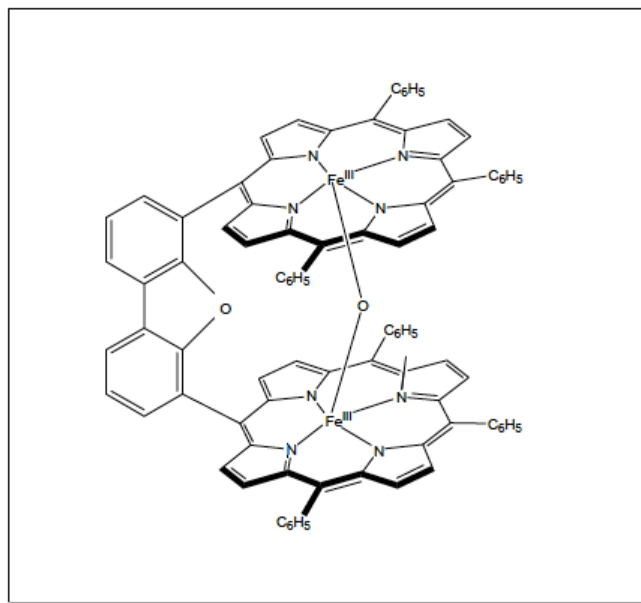
#### 1.4. Photocatalytic Aerobic Oxidations

In general terms, photocatalysis is the use of light to induce chemical transformations on organic or inorganic substrates that are transparent in the wavelength range employed.<sup>24-26</sup> Radiation is absorbed by a photocatalyst whose electronically excited states induce electron- or energy-transfer reactions that, in turn, trigger the chemical reactions desired. Examples of photocatalytic processes employed for synthetic purposes are oxidation and reduction processes, isomerization reactions, C- H bond activations, and C- C and C- N bond-forming reactions.<sup>27</sup>

The use of solar light as a reagent in oxidative catalysis is very much relevant to realizing innovative and economically advantageous processes for conversion of hydrocarbons into oxygenates, and at the same time, to move toward a “sustainable chemistry” that maximizes the “green” factor.<sup>27</sup> Three main reasons illustrate this: (i) solar light is a totally renewable source of energy; (ii) photochemical excitation requires milder conditions than thermal activation; (iii) and photochemical excitation allows one to conceive shorter reaction sequences and to minimize undesirable side reactions.<sup>27</sup> The second integral reagent employed in the oxygenation processes considered is the molecule of O<sub>2</sub>. In this connection, it is important to highlight that the search for new catalysts capable of inducing the oxofunctionalization of hydrocarbons with this environmentally friendly and cheap reagent represents a major target from the synthetic and industrial perspective.<sup>27</sup>



This work aims to extend the use of photocatalysis for the oxofunctionalization of hydrocarbons with molecular oxygen. In this context, we have an interest in photochemical generation of highly reactive metal-oxo intermediates that, upon oxidization of substrates, give low valent metal complexes and can be recycled for catalytic oxidations. One example of a catalytic aerobic oxidation driven by a photodisproportionation reaction employed a diiron(III)- $\mu$ -oxo bisporphyrin complex.<sup>5</sup> Also the photocatalytic oxidations of hydrocarbons using molecular oxygen as the oxygen source with no added reducing agent for the oxygen have been developed.<sup>6</sup> The low reactivity of the formed iron(IV)-oxo transients and poor quantum efficiency are serious obstacles that limit the use of iron porphyrins as practical photocatalysts, but the catalytic efficiency of diiron(III)- $\mu$ -oxo bisporphyrin systems was improved by Nocera and co-workers who employed “Pacman” ligand designs with organic spacer hinges serving to preorganize two iron centers in a cofacial arrangement Scheme 5.<sup>8,28,10,29</sup>



**Scheme 5.** “Pacman” diiron(III)- $\mu$ -oxo-bisporphyrin complex

This study has discovered that ruthenium(IV)  $\mu$ -oxo bisporphyrin complexes catalyzed efficient aerobic oxidation of alkenes and activated hydrocarbons by using visible light and atmospheric oxygen as oxygen source. The observed photocatalytic oxidation is ascribed to a photodisproportionation mechanism to afford a putative porphyrin-ruthenium(V)-oxo species that can be directly observed and kinetically studied by laser flash photolysis methods.<sup>30,31</sup>

## II. EXPERIMENTAL SECTION

### 2.1. Materials & Chemicals

All the organic solvents for synthesis and purification, including acetonitrile, methylene chloride, chloroform, hexane, ethyl acetate, methanol, acetone, ethanol and carbon tetrachloride, were of analytical grade and used as received without further purification. All reactive substrates for kinetic and photocatalytic studies were the best available purity from Aldrich Chemical Co., including, *cis*-cyclooctene, styrene, diphenylmethane, cyclohexene, ethylbenzene, deuterium ethylbenzene-*d*<sub>10</sub>, triphenylphosphine, benzophenone, xanthenes, xanthinol, 1-phenylethanol, cumene, norbornylene, 1,2-dihydronaphthalene and cyclohexene. The pyrrole was obtained from Aldrich Chemical Co. and freshly distilled before use. 1,2,4-Trichlorobenzene was obtained from Sigma Aldrich and used as solvent and internal standard in gas chromatography analysis. Iodobenzene diacetate, iodosobenzene (PhIO), benzaldehyde,  $\alpha,\alpha,\alpha$ -trifluoro-*p*-tolualdehyde, 4-methoxybenzaldehyde, triruthenium dodecacarbonyl, decahydronaphthalene (decalin), *meta*-chloroperoxybenzoic acid, 5,10,15,20-tetrakis(pentafluorophenyl)porphyrin [H<sub>2</sub>(F<sub>20</sub>-tpp)], anthracene, silver nitrate, silver perchlorate, silver chlorate, chloroform-*d*, acetonitrile-*d*<sub>3</sub>, hydrogen peroxide, *tert*-butylhydroperoxide, deuterium hydrogen oxide, aluminum oxide were purchased from Sigma-Aldrich and also used as received.

### 2.2 Photocatalytic Oxidation Studies.

*trans*-Dioxoruthenium(VI) porphyrin and bis-porphyrin-ruthenium(IV)  $\mu$ -oxo dimer complexes were evaluated as the photocatalyst in the aerobic oxidation reactions. A Rayonet photoreactor (RPR-100) with a wavelength range (400-500 nm,  $\lambda_{\text{max}}$  at 420

nm) from ca. 300 W visible lamps (RPR-4190 Å~12) was used for the photocatalytic reactions. The photochemical reactions typically employed 0.25 – 0.5  $\mu$ mol of  $[\text{Ru}^{\text{IV}}(\text{Por})\text{OH}]_2\text{O}$  in 5 mL of solution containing 2 to 4 mmol of substrate. In most cases, 5 ~ 10 mg of anthracene was added to enhance the catalytic activity. Dry oxygen or air gas was bubbled through the solution as it was irradiated. After 24 hours of photolysis with visible light ( $\lambda_{\text{max}} = 420$  nm), a known amount of 1,2,4-trichlorobenzene was added as an internal standard for GC analysis. Aliquots of the reaction solution were analyzed by GC HP 5890 and GC/MS spectrometry (Agilent GC6890/MS5973) to determine the products and yields (as measured against an internal standard). Product identification is based on the commercially available authentic standards. Turnover number (TON) is calculated based on the following definition:

$$\text{TON} = \text{moles of products} / \text{moles of catalyst}$$

### 2.3 Kinetic Isotope Effect (KIE) Study.

A solution containing equal amounts of two substrates, i.e., ethylbenzene (0.5 mmol) and ethylbenzene-  $d_{10}$  (0.5 mmol), ruthenium(IV) catalyst (0.25  $\mu$ mol), and an internal standard of 1,2,4-trichlorobenzene (0.2 mmol) was prepared (volume = 5 mL). The standards were shown to be stable to the oxidation conditions in control reactions. The mixture was irradiated with visible light under an aerobic atmosphere at ambient temperature for 48 hours. The amounts of substrates before and after the reactions were determined by GC (FID, DB-5). Relative rate constants for oxidations (KIE) were determined based on the average concentrations of the substrates, which introduces a

minor error (<5%). The value reported in the text is the average of two runs.

#### 2.4. Physical Measurements

UV-vis spectra were recorded on an Agilent 8453 spectrophotometer and processed using SigmaPlot software. Gas Chromatograph analyses were conducted on a Hewlett-Packard model HP 5890 Series II equipped with a flame ionization detector (FID) with DB-5 capillary column. The GC system is coupled with HP 7673 GC/SFC auto sample injector. Quantification of gas chromatographic fractions was conducted using an Agilent 3396 Series III integrator. <sup>1</sup>H-NMR was performed on a JEOL ECA-500 MHz spectrometer, all peaks are relative to TMS.

#### 2.5. Reagents Purification

The distillation of pyrrole was conducted according to the following procedure. Approximately 25 mL of pyrrole was measured using a graduated cylinder and then added to a 50 ml round-bottom flask containing a magnetic stir bar. The round-bottom flask was fitted with a water-jacketed condenser short-path from Chem Glass. Heating was achieved with a variac and spherical heating mantle. Since the boiling point of pyrrole is around 129 °C, all the distillate collected below that temperature was discarded. The freshly distilled colorless pyrrole was directly used in synthesis of the free porphyrin ligand.

### III. PHOTOCATALYTIC AEROBIC OXIDATION VIA A BIS-PORPHYRIN-RUTHENIUM(IV) $\mu$ -OXO DIMER

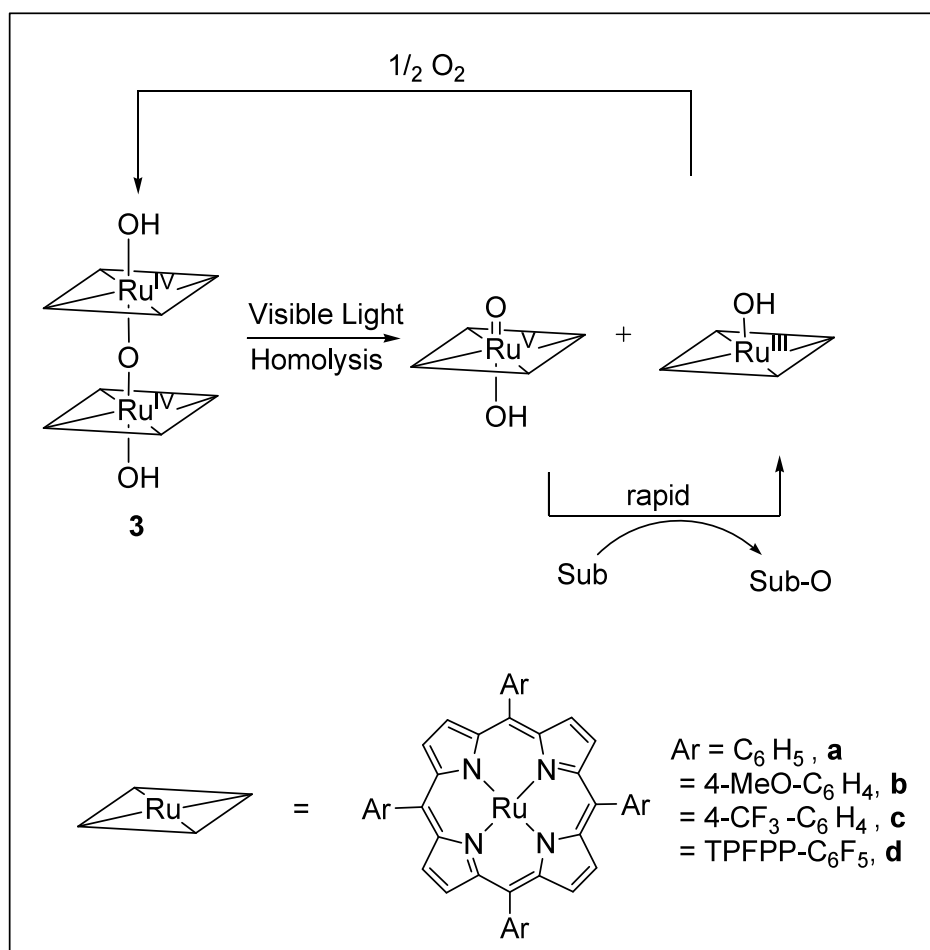
#### 3.1. Introduction

Selective oxidation is a significant technology for the synthesis of high value chemicals in the pharmaceutical and petrochemical industries, but the oxidations are among the most problematic processes to control.<sup>32</sup> Many stoichiometric oxidants with heavy metals are expensive and/or toxic and impractical. The ideal green catalytic oxidation process would use atmospheric oxygen as the primary oxygen source, recyclable catalysts in nontoxic solvents and an inexpensive energy source.<sup>33</sup> In this context, we have aimed to photochemically generate highly reactive metal-oxo intermediates that, upon oxidization of substrates, give low-valent metal complexes and can be recycled for catalytic oxidations.

Among the high-valent metal-oxo species, metal(V)-oxo complexes deserve special attention because they are highly reactive, although rare and elusive. The known porphyrin manganese(V)-oxo complexes showed higher reactivity than well-studied iron(IV)-oxo porphyrin radical cation analogues.<sup>34</sup> A recent paper by Collins et al. reported spectroscopic evidence for an oxoiron(V) complex supported by a tetraanionic ligand that showed unprecedented reactivity.<sup>35</sup> Putative porphyrin and corrole-iron(V)-oxo transients produced by laser flash photolysis methods displayed appropriately high levels of reactivity expected for iron(V)-oxo species,<sup>36,37</sup> and recently a photodisproportionation of a bis-corrole-iron(IV)  $\mu$ -oxo dimer apparently gave the same type of corrole-iron(V)-oxo transient in a system that has potential for light-driven oxidation catalysis.<sup>38</sup>

In this section, we explore the applicability of ruthenium porphyrins for the

aerobic oxidation of hydrocarbons using visible light and atmospheric oxygen in sequences employing photo-disproportionation reactions. As shown in Scheme 6, the catalytic sequences were proposed via a photo-disproportionation pathway to give a putative ruthenium(V)-oxo species that serves as the actual oxidizing agent.



**Scheme 6.** Photocatalytic aerobic oxidation by a bis-porphyrin-ruthenium(IV)  $\mu$ -oxo dimer.

### 3.2. Synthesis and Spectroscopic Characterization of *meso*-Tetraphenylporphyrin H<sub>2</sub>Por (**1a-c**)

According to a known literature method described in Scheme 7,<sup>39</sup> a 500 mL round bottom flask was filled with propionic acid (350 mL). Immediately following was the addition of freshly distilled pyrrole (5 mL, 7.2mmol) and benzaldehyde (7 mL, 69mmol). The reaction was heated to reflux with stirring for 30 min, then cooled to room temperature and filtered under vacuum. The resulting filter cake was washed thoroughly with methanol, and the resulting purple crystals were dried under vacuum. The desired *meso*-tetraphenylporphyrin (**1a**) product with a 19.4% yield was confirmed by UV-Vis and <sup>1</sup>H-NMR spectroscopy (Figure 3 and 4), and was in agreement to those reported in the literature.<sup>39</sup>

[H<sub>2</sub>TPP] (**1a**) UV-Vis (CH<sub>2</sub>Cl<sub>2</sub>)  $\lambda_{\text{max}}$ /nm: 420 (Soret), 448, 515, 552, 595, 648.

<sup>1</sup>H-NMR (500MHz, CDCl<sub>3</sub>):  $\delta$ , ppm: 8.85 (pyrrolic H, 8H), 8.21 (s, 12 H), 7.76 (s 8H), -2.81(s, 8H)

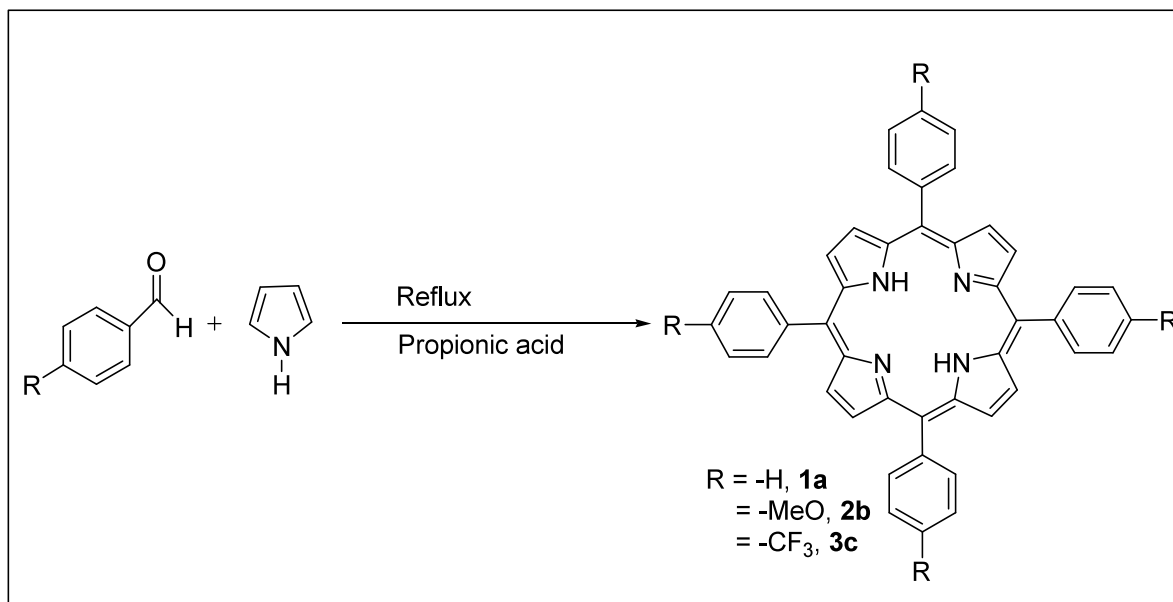
In a similar fashion, another two porphyrins, formulated as [H<sub>2</sub>(4-MeO-TPP)] (**1b**) and [H<sub>2</sub>(4-CF<sub>3</sub>-TPP)] (**1c**), were made and characterized by UV-Vis and <sup>1</sup>H NMR spectroscopies.

[H<sub>2</sub>(4-MeOTPP)] (**1b**) Yield = 20.1%. UV-Vis (CH<sub>2</sub>Cl<sub>2</sub>)  $\lambda_{\text{max}}$ /nm: 422 (Soret), 454, 519.

<sup>1</sup>H-NMR (500MHz, CDCl<sub>3</sub>):  $\delta$ , ppm: 8.81 (s, pyrrolic H, 8H), 8.10,(d, 8H) 7.51(d, 8H), 4.1(s, MeO, 3H).

[H<sub>2</sub>(4-CF<sub>3</sub>TPP)] (**1c**) Yield = 21.9%.  $\lambda_{\text{max}}$ /nm: 418 (Soret), 514, 549. <sup>1</sup>H-NMR (500MHz, CDCl<sub>3</sub>):  $\delta$ , ppm: -2.88 (s inner H NH) 8.85 (s, pyrrolic H, 8H), 8.60 (d, 8 H) 7.76 (d 8H)





**Scheme 7.** Synthesis of porphyrin free ligands (**1**)

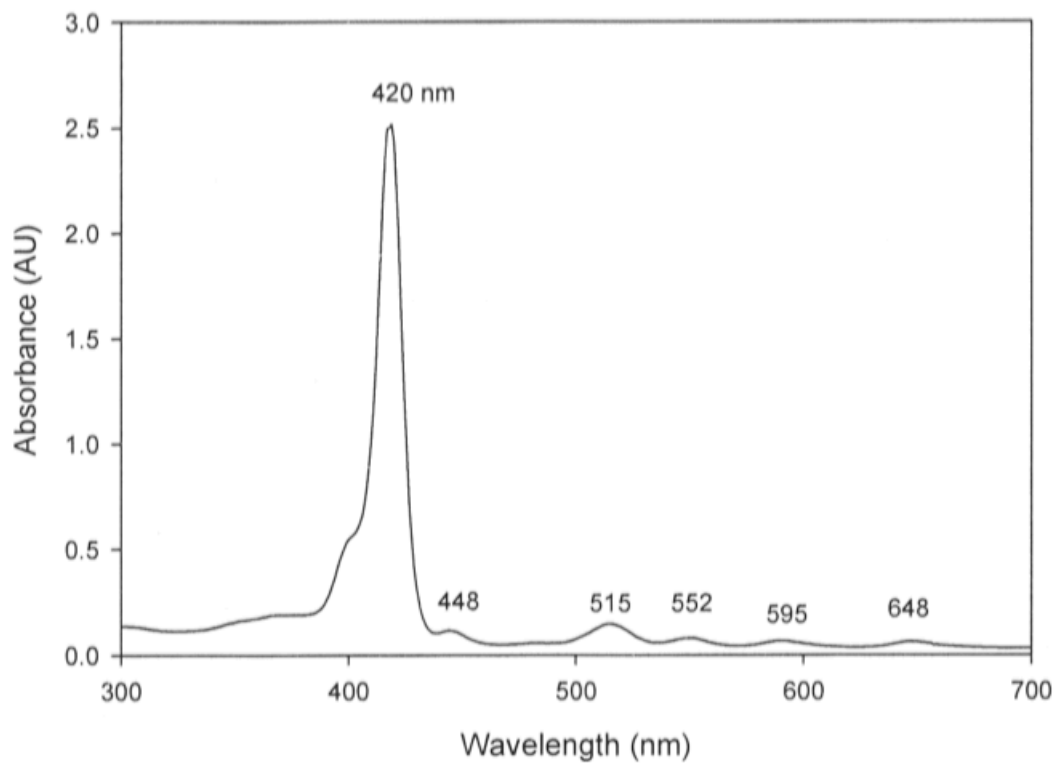


**Figure 3.** UV-Vis spectroscopy of H<sub>2</sub>TPP (1a) CH<sub>2</sub>Cl<sub>2</sub>.

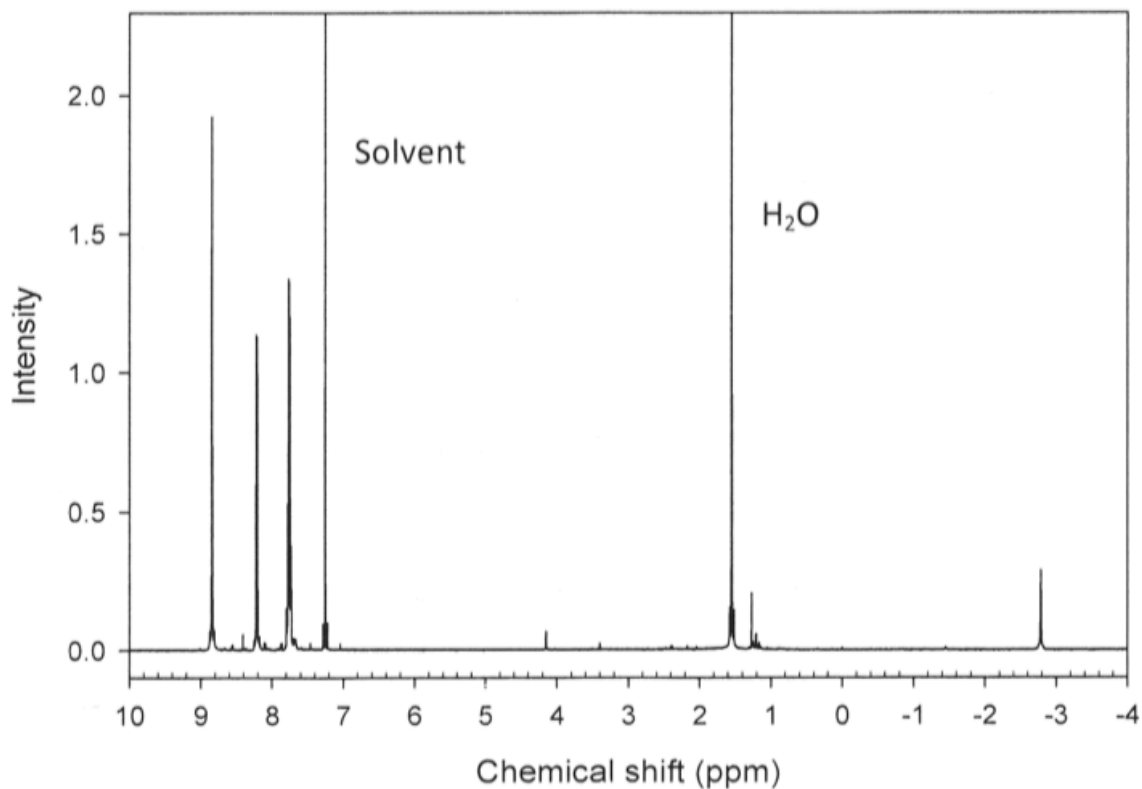
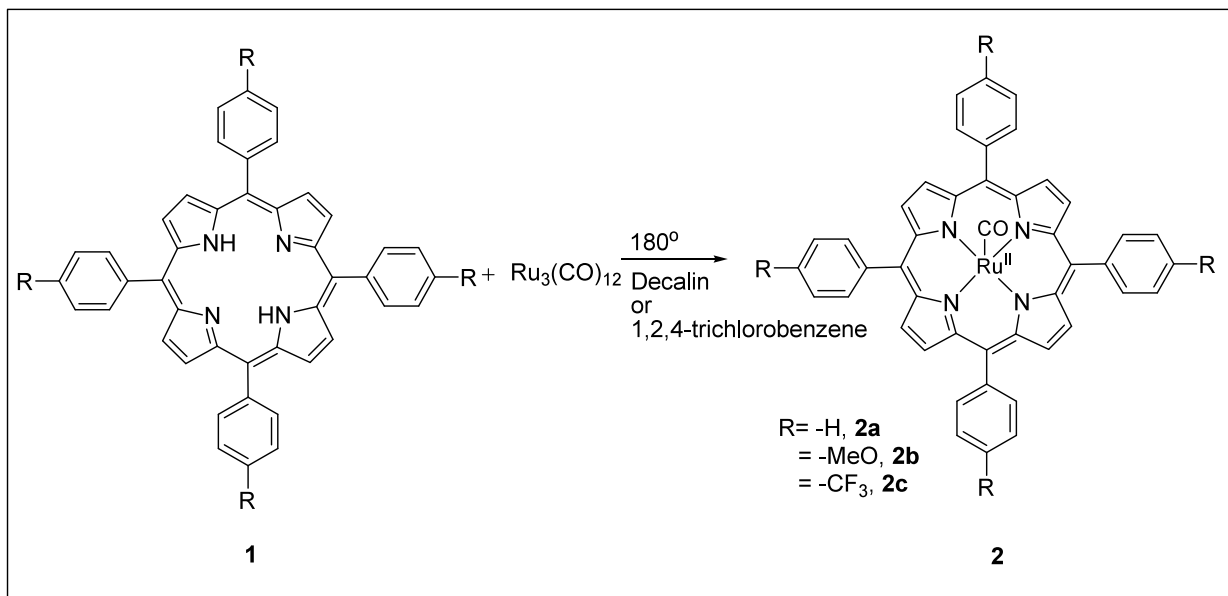


**Figure 4.** <sup>1</sup>H-NMR spectroscopy of H<sub>2</sub>TPP (1a) in CDCl<sub>3</sub>.

### 3.3.1. Synthesis and Characterization of Carbonyl Ruthenium(II) Porphyrin Complexes (2).

The carbonyl ruthenium(II) porphyrin complexes were synthesized according to the literature methods described by Che and co-workers (Scheme 8 ).<sup>40</sup> The reaction is solvent and temperature dependent. For the carbonyl (5, 10, 15, 20 tetraphenyl porphyrinato)-ruthenium(II), abbreviated as  $[\text{Ru}^{\text{II}}(\text{CO})\text{TPP}]$  (**2a**), decalin, a non-polar solvent, was used to provide a refluxing temperature at 180°C. The same conditions were used in the synthesis of the electronically similar  $[\text{Ru}^{\text{II}}(\text{CO})(4\text{-MeOTPP})]$  (**2b**). However, 1,2,4-trichlorobenzene, which is a more polar solvent than decalin, was used for the synthesis of the more electron deficient complex, carbonyl (5,10,15,20-tetrapenta fluorophenylporphyrinato)-ruthenium(II) abbreviated as  $[\text{Ru}^{\text{II}}(\text{CO})\text{TPFPP}]$  (**2d**). This method was also employed in the synthesis of  $[\text{Ru}^{\text{II}}(\text{CO})(4\text{-CF}_3\text{-TPP})]$  (**2c**). The use of more polar 1,2,4-trichlorobenzene at a higher temperature (220°C) in the synthesis of **2d** resulted in a better yield compared to the use of the non-polar decalin (~ 10% yield). Also, the synthesis of **2d** in 1,2,4-trichlorobenzene resulted in a much higher yield (93%) than earlier procedures using *o*-dichlorobenzene (55% yield).<sup>40</sup>



**Scheme 8.** Synthesis of  $[\text{Ru}^{\text{II}}(\text{CO})\text{Por}]$  (**2**).

### 3.3.2. Preparation of Carbonyl (5,10,15,20-tetraphenylporphyrinato) Ruthenium(II)

#### $[\text{Ru}^{\text{II}}(\text{CO})\text{TPP}]$ (**2a**).

A mixture of  $[\text{Ru}_3(\text{CO})_{12}]$  (100 mg) and **1a** (100 mg) in decalin (50 mL) was refluxed and stirred for an hour and a half at a temperature of about  $180^\circ\text{C}$  (Scheme 8). The mixture was cooled to room temperature and an alumina chromatography was used for product purification. An excess amount of hexane was first used to remove all decalin. Dichloromethane was then used to remove free ligand. A mixture of acetone and dichloromethane (1:1, v/v) was used to elute the desired product, **2a**. The solvent was removed by rotary evaporation and a brick-red solid (~100 mg) was obtained with a yield of 90 %.

The UV-Vis spectrum of  $[\text{Ru}^{\text{II}}(\text{CO})\text{TPP}]$  in dichloromethane ( $\text{CH}_2\text{Cl}_2$ ) (Figure 5) shows a strong signal at 411 nm (Soret band) and a less intense signal at 532 nm, (Q band).  $^1\text{H-NMR}$  (500MHz,  $\text{CDCl}_3$ ):  $\delta$ , ppm: 8.68 (s, pyrrolic H, 8H), 8.2 (d, ArH, 8H)

7,46(s, 12H) (Figure 6). In a similar way, complexes **2b** and **2c** were made and characterized by UV-Vis and  $^1\text{H}$ -NMR spectroscopy.

$[\text{Ru}^{\text{II}}(\text{CO})(4\text{-MeOTPP})]$  (**2b**) Yield = 90% UV-Vis ( $\text{CHCl}_2$ )  $\lambda_{\text{max}}/\text{nm}$ : 415 (Soret), 532.

$^1\text{H}$ -NMR (500MHz,  $\text{CDCl}_3$ ):  $\delta$ , ppm: 8.61 (s, pyrrolic H, 8H), 8.2 (d, 8H) 7.5 (d, 8H), 4.2 (s, MeO, 3H).

$[\text{Ru}^{\text{II}}(\text{CO})(4\text{-CF}_3\text{-TPP})]$  (**2c**) Yield = 91%. UV-Vis ( $\text{CH}_2\text{Cl}_2$ )  $\lambda_{\text{max}}/\text{nm}$ : 418 (Soret), 510.

$^1\text{H}$ -NMR (500MHz,  $\text{CDCl}_3$ ):  $\delta$ , ppm: 8.69 (s, 8H, pyrrolic), 8.0 (s, ArH, 8H).

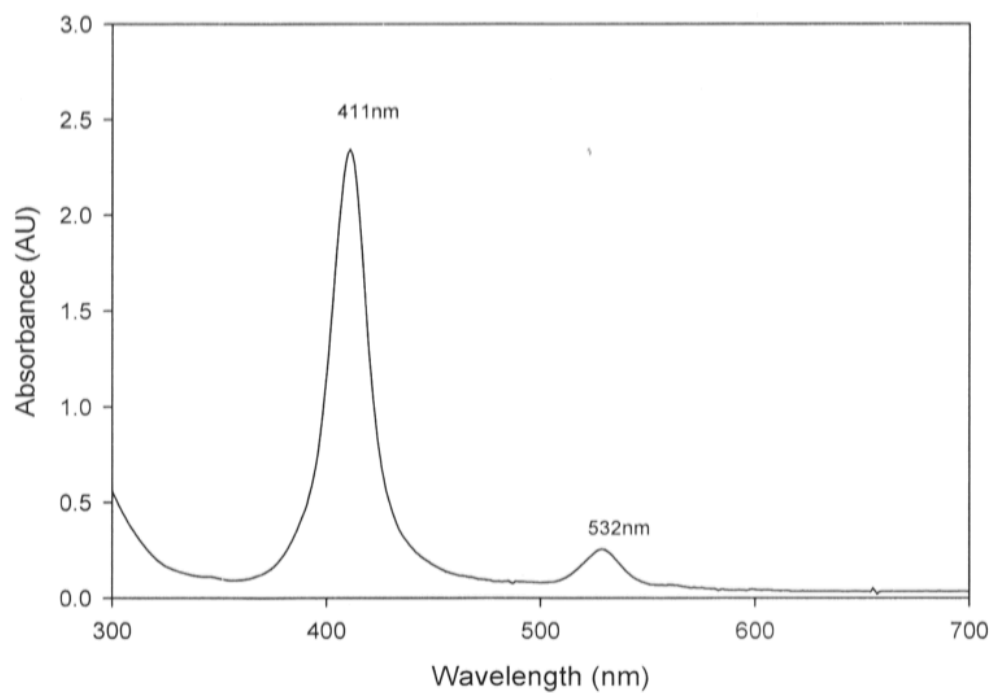


**Figure 5.** UV-Vis of  $[\text{Ru}^{\text{II}}(\text{CO})\text{TPP}]$  in  $\text{CH}_2\text{Cl}_2$  (**2a**).

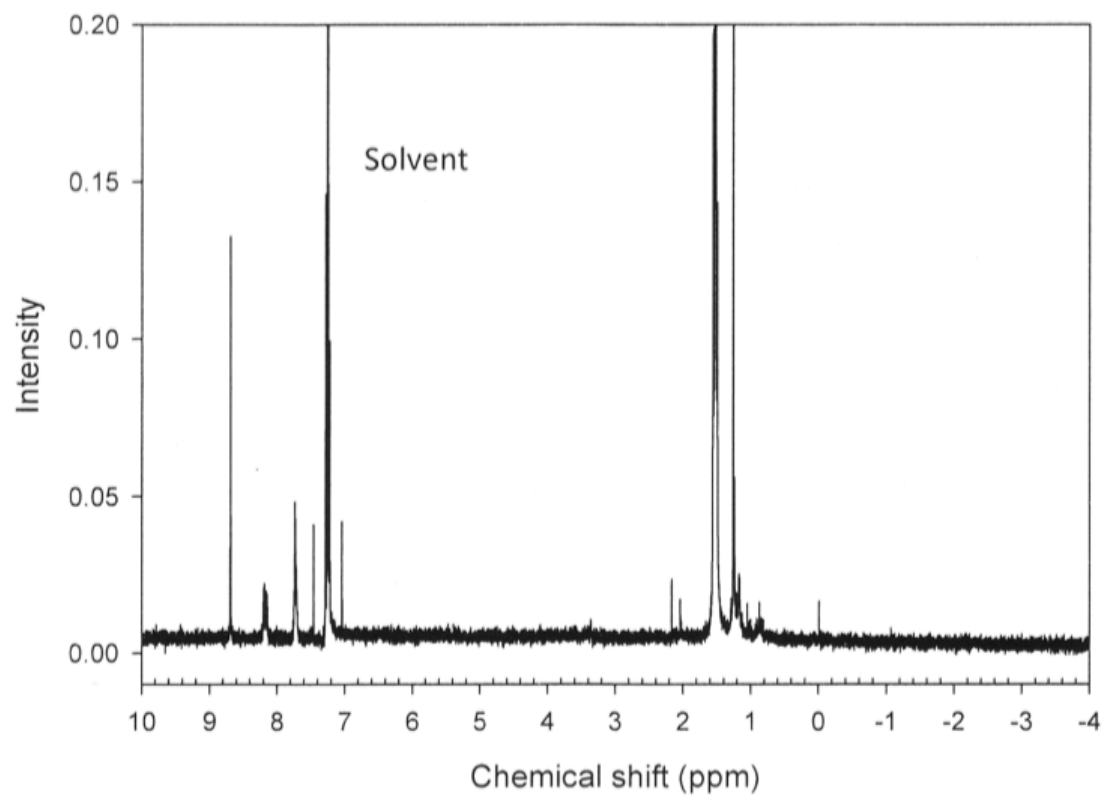


**Figure 6.**  $^1\text{H}$ -NMR of  $[\text{Ru}^{\text{II}}(\text{CO})\text{TPP}]$  (**2a**).

### 3.3.3 Preparation of Carbonyl (5,10,15,20-tetrakis(pentafluorophenyl)porphyrinato)

#### Ruthenium(II) [Ru<sup>II</sup>(CO)TPFPP] (**2d**)

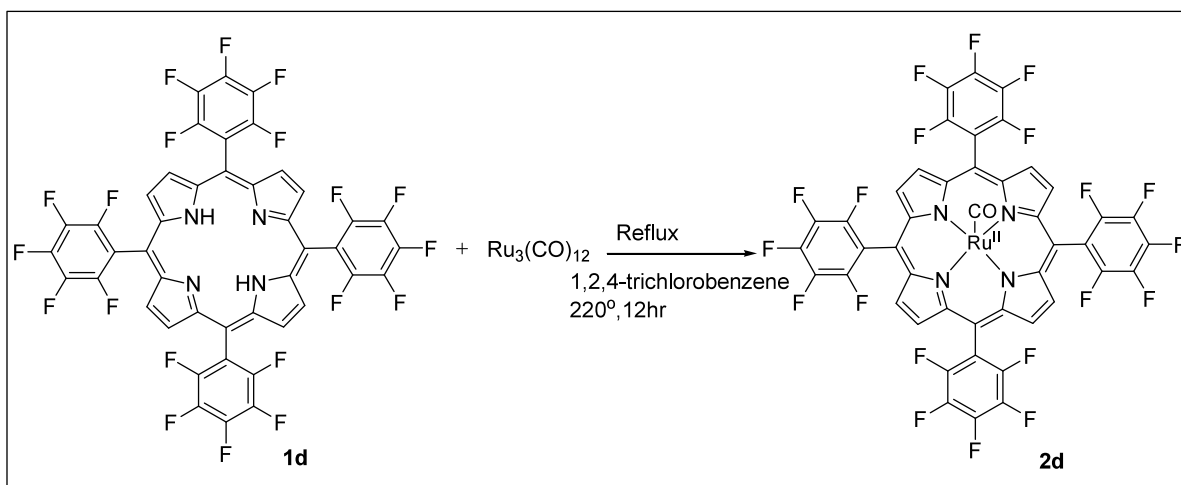
A mixture of [Ru<sub>3</sub>(CO)<sub>12</sub>] (100 mg) and **1d** (100 mg) in freshly distilled 1,2,4-trichlorobenzene (50 mL) was refluxed overnight (Scheme 9). The solvent of the mixture was then removed under vacuum, and the residue obtained was chromatographed on alumina column. A mixture of dichloromethane and hexane (1:1 v/v) was used to elute the unreacted free ligand and impurities. The brick red band containing the desired product was then eluted with a mixture of dichloromethane and acetone (1:1,v/v). The crude product was recrystallized from a CH<sub>2</sub>Cl<sub>2</sub>/*n*-hexane mixture to give a dark purple solid product. The resulting crystals were air dried to yield 93% of product, **2d**.

The UV-vis spectrum of [Ru<sup>II</sup>(CO)TPFPP] in chloroform (Figure 7) shows a strong signal at 404 nm for the Soret band and a weak signal at 524 nm for the Q band.

<sup>1</sup>H NMR (CDCl<sub>3</sub>): δ 8.76 (pyrrolic H, 8H) (Figure 8).

[Ru<sup>II</sup>(CO)TPFPP] (**2d**) Yield = 93%. UV-Vis (CH<sub>2</sub>Cl<sub>2</sub>) λ<sub>max</sub>/nm: 404 (Soret), 524.

<sup>1</sup>H-NMR (500MHz, CDCl<sub>3</sub>): δ, ppm: 8.71 (s, 8H,pyrrolic).



**Scheme 9.** Synthesis of [Ru<sup>II</sup>(CO)TPFPP] (**2d**).

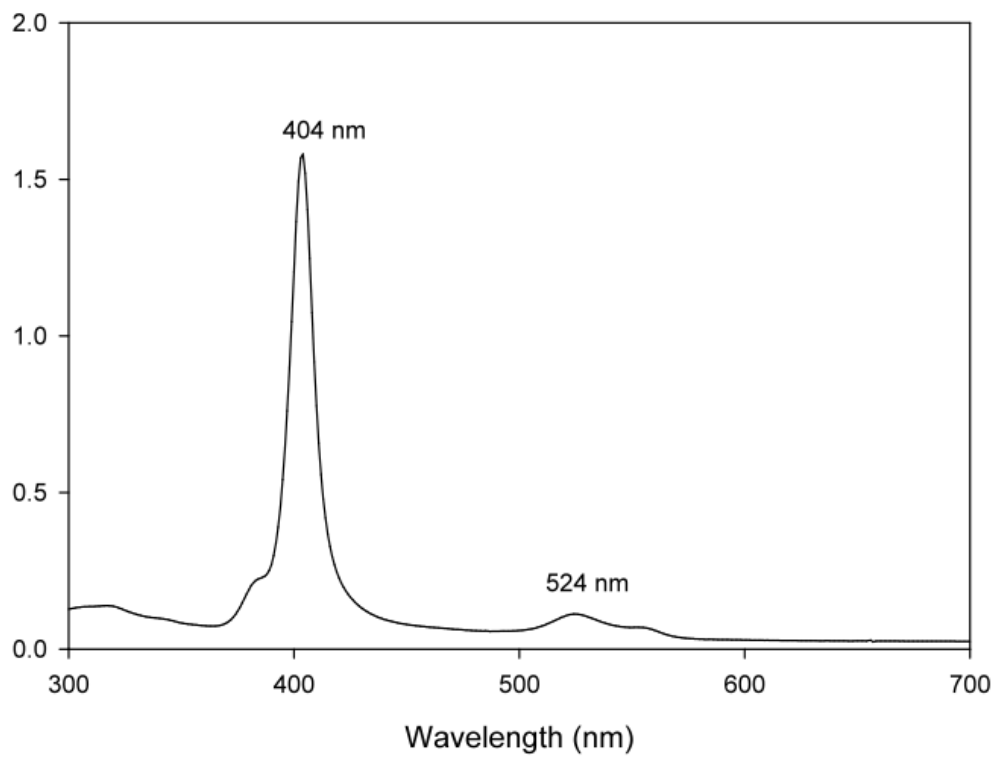


**Figure 7.** UV-Vis of  $[\text{Ru}^{\text{II}}(\text{CO})\text{TPFPP}]$  (**2d**) in  $\text{CHCl}_3$ .

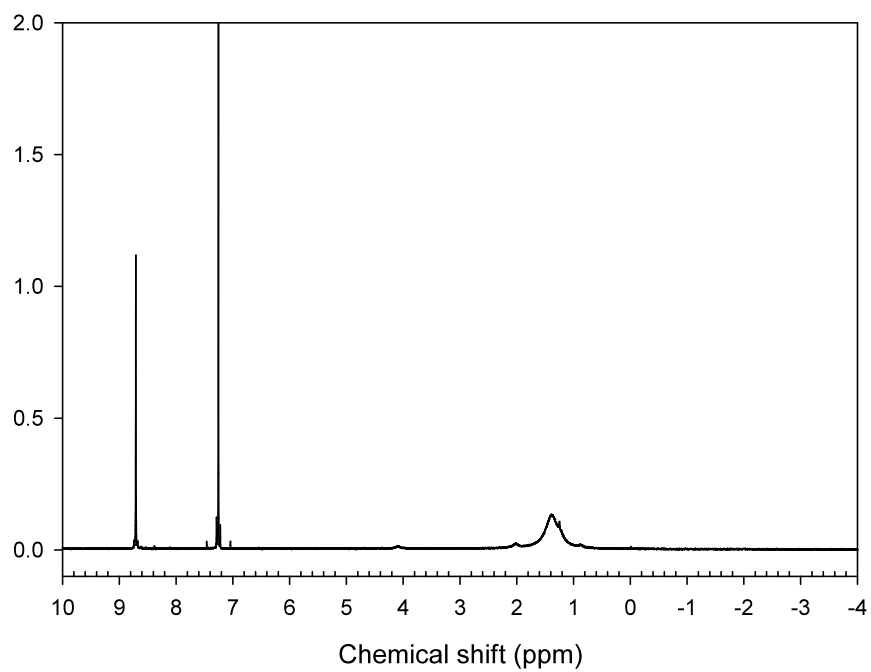


**Figure 8.** of  $[\text{Ru}^{\text{II}}(\text{CO})\text{TPFPP}]$  (**2d**) in  $\text{CDCl}_3$ .



### 3.4.1 Synthesis and Characterization of Bis-Porphyrin-Ruthenium(IV) $\mu$ -Oxo Dimers (**3**)

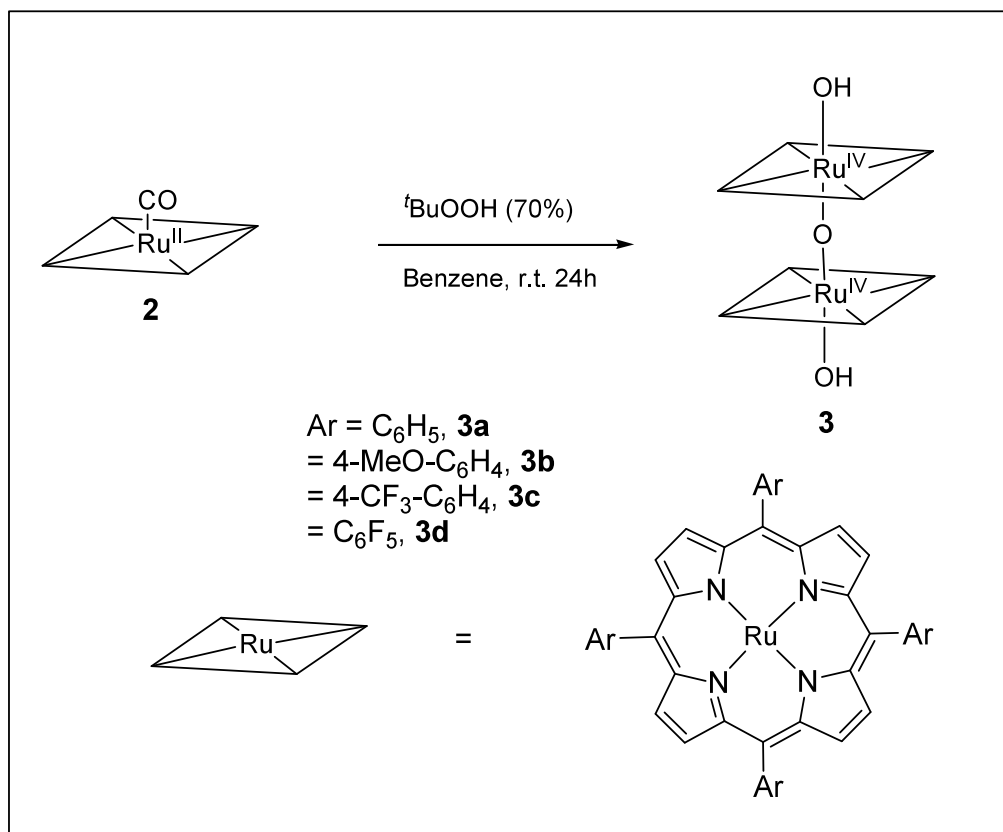
According to the known method described by Sugimoto and co-workers,<sup>41</sup> the bisporphyrin-ruthenium(IV)  $\mu$ -oxo dimer (**3**) was synthesized by the following procedure (Scheme 10). Ru<sup>II</sup>(CO)(Por) (**2**) (50 mg) was placed in a 100 mL round-bottom flask with benzene (50 mL) and 70% aqueous *tert*-butyl hydroperoxide (0.5 mL). The reaction mixture was stirred at room temperature until the color of the solution turned from orange red to dark brown. After removal of the benzene under reduced pressure, the residual solid was chromatographed on an alumina with dichloromethane as an eluant, achieving (~90%) yield. The desired dimer bis-porphyrin-ruthenium(IV)  $\mu$ -oxo dimer [Ru<sup>IV</sup>(Por)(OH)]<sub>2</sub>O (**3**) was characterized by UV-vis (Figure 9) and <sup>1</sup>H-NMR (Figure 10), consistent with the literature reported.<sup>41</sup>

[Ru<sup>IV</sup>(TPP)OH]<sub>2</sub>O (**3a**) Yield= 90%. UV-Vis (CH<sub>2</sub>Cl<sub>2</sub>)  $\lambda_{\text{max}}$ /nm: 393 (Soret), 552 (Q band). <sup>1</sup>H-NMR (500MHz, CDCl<sub>3</sub>):  $\delta$ , ppm: 8.9 (d, H<sub>o</sub>), 8.6 (s, pyrrolic H), 7.9, 7.4 (d, H<sub>m,p</sub>), -3.9 (axial ligand, OH)

[Ru<sup>IV</sup>(4-MeO-TPP)OH]<sub>2</sub>O (**3b**) Yield= 90%. UV-Vis (CH<sub>2</sub>Cl<sub>2</sub>)  $\lambda_{\text{max}}$ /nm: 398 (Soret), 560 (Q band). <sup>1</sup>H-NMR (500MHz, CDCl<sub>3</sub>):  $\delta$ , ppm: 8.7 (d, H<sub>o</sub>), 8.6 (s, pyrrolic H) 7.5 (d, H<sub>m</sub>), 4.2 (CH<sub>3</sub> MeO), -4.0 (axial ligand, OH)

[Ru<sup>IV</sup>(4-CF<sub>3</sub>-TPP)OH]<sub>2</sub>O (**3c**) Yield= 90%. UV-Vis (CH<sub>2</sub>Cl<sub>2</sub>)  $\lambda_{\text{max}}$ /nm: 394 (Soret), 596 (Q band). <sup>1</sup>H-NMR (500MHz, CDCl<sub>3</sub>):  $\delta$ , ppm: 8.6 (d, H<sub>o</sub>) 8.5 (s, pyrrolic H), 8.0 (d, H<sub>m</sub>), -4.1 (axial ligand, OH)

[Ru<sup>IV</sup>(TPFPP)OH]<sub>2</sub>O (**3d**) Yield= 90%. UV-Vis (CH<sub>2</sub>Cl<sub>2</sub>)  $\lambda_{\text{max}}$ /nm: 392 (Soret), 560 (Q band). <sup>1</sup>H-NMR (500MHz, CDCl<sub>3</sub>):  $\delta$ , ppm: 8.90 (s, pyrrolic H), -4.1 (axial ligand, OH)



**Scheme 10.** Synthesis of  $[\text{Ru}^{\text{IV}}(\text{Por})(\text{OH})]_2\text{O}$  (**3**)

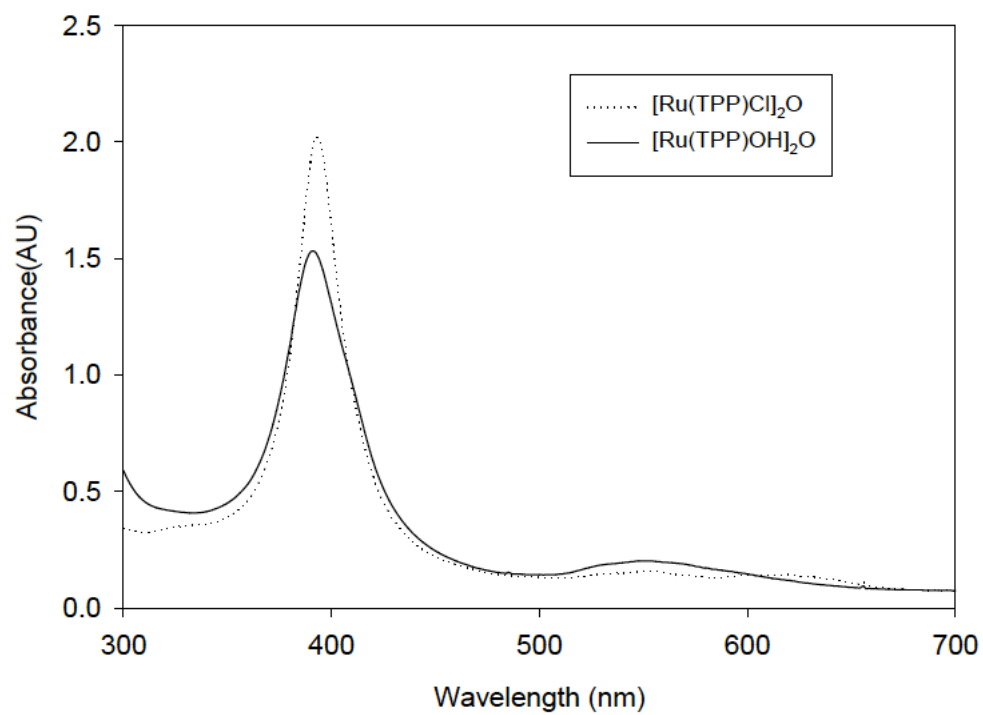


**Figure 9.** UV-Vis of  $[\text{Ru}^{\text{IV}}(\text{TPP})]_2\text{O}$  in  $\text{CHCl}_3$  (**3a**).

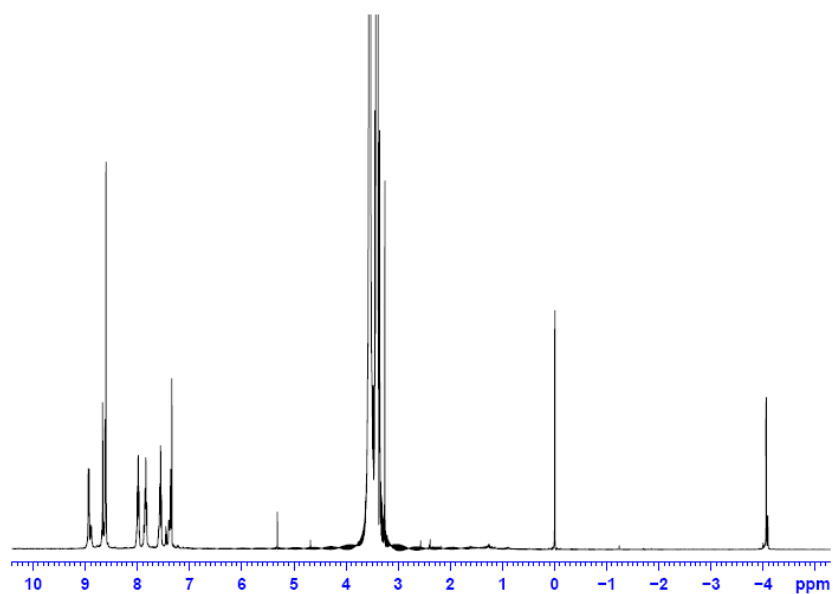


**Figure 10.**  $^1\text{H}$ -NMR of  $[\text{Ru}^{\text{IV}}(\text{TPP})]_2\text{O}$  (**3a**) in  $\text{CDCl}_3$ .

### 3.4.2 Photocatalytic Aerobic Oxidation by a Bis-Porphyrin- Ruthenium(IV) $\mu$ -Oxo Dimer

#### (3).

When dissolved in acetonitrile solution, complexes **3** were thermally stable to hydrocarbons, but irradiation with light ( $\lambda_{\text{max}} = 420 \text{ nm}$ ) of anaerobic solutions of complexes **3** in the presence of excess triphenylphosphine (50 mM) resulted in changes in the absorption spectra with isosbestic points (Figure 11). The shift in the absorption spectra presents direct evidence of photo-disproportionation of the bis-porphyrin-ruthenium(IV)  $\mu$ -oxo dimer. Similar spectral changes were previously observed upon the photolyses of diiron(III)- $\mu$ -oxo bisporphyrin complexes in the presence of  $\text{Ph}_3\text{P}$ . According to previous studies by Collman and coworkers,<sup>42</sup> the product formed with  $\lambda_{\text{max}}$  at 430 nm was assigned as  $\text{Ru}^{\text{II}}(\text{TPP})(\text{PPh}_3)_2$ . The spectral signature of  $\text{Ru}^{\text{II}}(\text{TPP})(\text{PPh}_3)_2$  was further confirmed by production of the same species in the known experiment of the  $\text{Ru}^{\text{VI}}(\text{TPP})\text{O}_2$  with  $\text{Ph}_3\text{P}$ .<sup>42</sup>

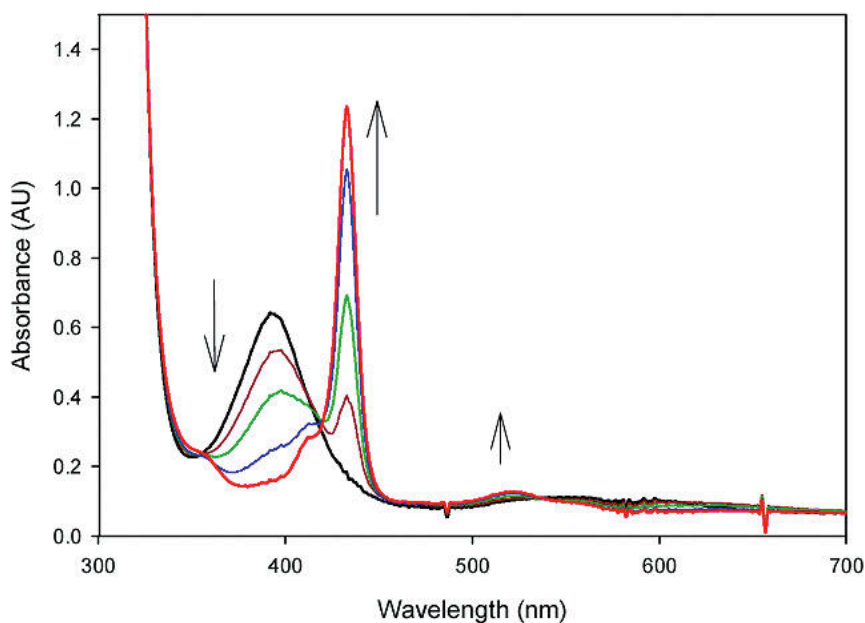


**Figure 11.** UV-vis spectral change of **3a** ( $6 \times 10^{-6} \text{ M}$ ) in the presence of excess  $\text{Ph}_3\text{P}$  (50

mM) upon irradiation with a 300-W visible lamp ( $\lambda_{\text{max}}$  420 nm) in anaerobic CH<sub>3</sub>CN solution. The spectra were recorded at  $t = 0, 2, 4, 6,$  and 10 min.

Metalloporphyrins are known to display superior oxidative robustness. A series of ruthenium(IV)- $\mu$ -oxo bisporphyrins was evaluated in the aerobic oxidation of *cis*-cyclooctene (Table 1). The reactions were carried out with 0.5  $\mu$ mol of catalyst in 5 mL of oxygen-saturated solution containing 4 mmol of *cis*-cyclooctene. After 24 h of photolysis with visible light ( $\lambda_{\text{max}} = 420$  nm), *cis*-cyclooctene oxide was obtained as the only identifiable oxidation product (> 95% by GC) with ca. 220 TON of catalyst **3a** (entry 1). The trend in the TONs roughly paralleled irradiation times. Control experiments showed that no epoxide was formed in the absence of either the catalyst or light. The results cannot be ascribed to the chemistry of singlet oxygen, which is characterized by efficient “ene” reactions of alkenes.<sup>43</sup> The use of other solvents instead of CH<sub>3</sub>CN, or air as oxygen source (data not shown), resulted in reduced TONs (entries 2- 4). Catalyst degradation was a problem with higher-energy light, but the use of UV irradiation increased catalytic activity (entry 5). It is interesting to note that the catalytic activity was enhanced by adding small amounts of anthracene (entries 6 and 9). Quite surprisingly, the axial ligand on the metal had a significant effect, and the [Ru<sup>IV</sup>(TPP)Cl]<sub>2</sub>O (entry 7) resulted in a much lower activity compared to [Ru<sup>IV</sup>(TPP)OH]<sub>2</sub>O. The substituent in the porphyrin ligand gave a noticeable effect on the catalytic activity (entries 1, 8, 10, and 11), with the most electron-demanding system, namely [Ru<sup>IV</sup>(TPFPP)OH]<sub>2</sub>O (**3d**), being the most efficient catalyst.

**Table 1.** Aerobic Photocatalytic Oxidation of *cis*-cyclooctene with Diruthenium(IV)  $\mu$ -Oxo Porphyrins<sup>a</sup>

Entry	Catalyst	Solvent	<i>t</i> /day	TON <sup>b,c</sup>
1	[Ru <sup>IV</sup> (TPP)OH] <sub>2</sub> O <b>3a</b>	CH <sub>3</sub> CN	1	220 ± 16
			2	460 ± 40
			3	640 ± 65
2		CHCl <sub>3</sub>	1	110 ± 18
3		C <sub>6</sub> H <sub>6</sub>	1	140 ± 6
4		THF	1	190 ± 10
5 <sup>d</sup>		CH <sub>3</sub> CN	1	340 ± 8
6 <sup>e</sup>		CH <sub>3</sub> CN	1	300 ± 35
7	[Ru <sup>IV</sup> (TPP)Cl] <sub>2</sub> O	CH <sub>3</sub> CN	1	70 ± 5
8	[Ru <sup>IV</sup> (4-CF <sub>3</sub> -TPP)OH] <sub>2</sub> O <b>3c</b>	CH <sub>3</sub> CN	1	250 ± 21
9 <sup>e</sup>		CH <sub>3</sub> CN	1	340 ± 9
10	[Ru <sup>IV</sup> (4-MeOTPP)OH] <sub>2</sub> O <b>3b</b>	CH <sub>3</sub> CN	1	190 ± 23
11	[Ru <sup>IV</sup> (TPFPP)OH] <sub>2</sub> O <b>3d</b>	CH <sub>3</sub> CN	1	300 ± 22

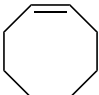
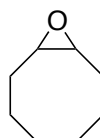
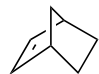
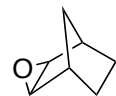
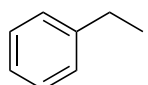
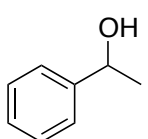
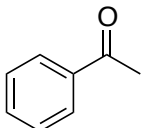
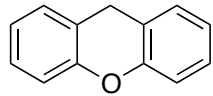
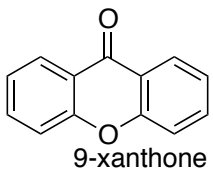
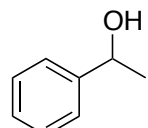
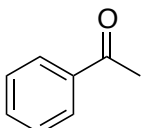
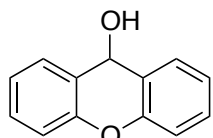
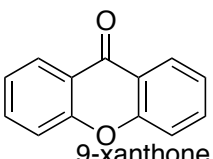
<sup>a</sup> The reaction was carried out in a Rayonet reactor, with 0.5  $\mu$ mol of catalyst in 5 mL of solvent containing 4 mmol of *cis*-cyclooctene. Oxygen saturated solutions were irradiated with visible light ( $\lambda_{\text{max}}$  ) 420 nm) or otherwise noted. Products were analyzed on an HP 5890 GC with a DB-5 capillary column employing an internal standard. <sup>b</sup> TON represents the total number of moles of product produced per mole of catalyst. All reactions were run three times, and the data reported are the averages with standard deviation (1 $\sigma$ ). <sup>c</sup> The major product was *cis*-cyclooctene oxide, detected in >95% yield. <sup>d</sup> UV-vis light ( $\lambda_{\text{max}}$  ) 350 nm). <sup>e</sup> 5 mg of anthracene was added as a photosensitizer.

### 3.4.3 Photocatalytic Aerobic Oxidation by a Bis-Porphyrin-Ruthenium(IV) $\mu$ -Oxo Dimer (3c)

The ruthenium(IV)  $\mu$ -oxo bisporphyrin (**3c**) was evaluated in the aerobic oxidation of a variety of organic substrates. The reactions were carried out in a similar way as described above. Table 2 lists the oxidized products and corresponding turnovers using **3c** as the photocatalyst. As shown in Table 2, the trend in the TONs roughly paralleled the substrate reactivity, and significant activity was observed with up to 3900 TON. After 24 hours photolysis, *cis*-cyclooctene and norbornene were oxidized to the corresponding epoxides with 200 ~ 250 TONs (entries 1 and 2). Activated hydrocarbons including ethylbenzene and xanthenes were oxidized to the corresponding alcohols and/or ketones from overoxidation with total TONs 560 and 2900, respectively (entries 3 and 4). It was noticeable that the oxidation of secondary benzylic alcohols gave the highest catalytic activities (entries 5 and 6).

Competitive catalytic oxidation of ethylbenzene and ethylbenzene- $d_{10}$  revealed a kinetic isotope effect (KIE) of  $k_H/k_D = 4.8 \pm 0.2$  at 298 K, similar to the KIE reported for the reaction of ethylbenzene with an electron-deficient iron(IV)-oxo porphyrin radical cation species.<sup>44</sup> The observed KIE is larger than those observed in autoxidation processes,<sup>45</sup> suggesting a nonradical mechanism that involves the intermediacy of ruthenium(V)-oxo species.

**Table 2.** Turnover Numbers for Alkenes and Benzylic C-H Oxidations Using [Ru<sup>IV</sup>(4-CF<sub>3</sub>-TPP)(OH)]<sub>2</sub>O (**3c**) as the photocatalyst.<sup>a</sup>

Entry	Substrate	Product	TON
1	 cis-cyclooctene	 cis-1,2-epoxycyclooctane	250 ± 21
2	 norbornene	 norbornene oxide	200 ± 40
3	 ethylbenzene	 1-phenylethanol	380 ± 41
		 acetophenone	180 ± 19
4	 xanthene	 9-xanthone	2900 ± 140
5	 1-phenylethanol	 acetophenone	3300 ± 240
6	 9-xanthenol	 9-xanthone	3900 ± 280

<sup>a</sup> The reactions were typically carried out with 0.5 mg of catalyst in the 10 mL oxygen-saturated solution containing 2 ~ 4 mmol of substrates. In most cases, 5 ~ 10 mg of anthracene was added to enhance the catalytic activity. After 24 hours of photolysis with visible light ( $\lambda_{\text{max}} = 420$  nm), a known amount of 1,2,4-trichlorobenzene was added as an



internal standard for GC analysis.<sup>b</sup> Determined for a 24 h photolysis ( $\lambda_{\text{max}} = 420 \text{ nm}$ ). The values reported are the average of 2~3 runs.

In summary, we have demonstrated that the ruthenium(IV)- $\mu$ -oxo bisporphyrins catalyzed efficient aerobic oxidation of alkenes and activated hydrocarbons using visible light and atmospheric oxygen. The observed photocatalytic oxidation is ascribed to a photo-disproportionation mechanism to afford a putative porphyrin- ruthenium(V)- oxo species that can be directly observed and kinetically studied by laser flash photolysis methods.

## IV. PHOTOCHEMICAL GENERATION OF *trans*-DIOXORUTHENIUM(VI) PORPHYRINS

### 4.1 Introduction

In both synthetic and natural catalysts, high-valent transition metal-oxo species have been implicated as the active oxidizing species.<sup>17, 46, 47</sup> In a typical catalytic reaction, however, the concentrations of active oxidants will not build up to concentrations that permit detection and direct kinetic studies. Moreover, a high valent metal-oxo species detected in a reaction might not be the true oxidant but is rather a precursor to the true oxidant that is formed in small, undetectable amounts.<sup>48</sup> The resulting lack of kinetic and mechanistic information complicates attempts to deduce the identities of the active oxidants. Indeed, most commonly, the nature of the active oxidants in homogeneous catalysis has been inferred indirectly from product studies.<sup>49-52</sup> The successful generation and characterization of the reactive metal-oxo species will allow a direct assessment of their reactivities and provide important insight into chemical modeling of the enzyme-like oxidants, and ultimately lead to catalyst development for the selective oxidation of organic substrates in large-scale industrial processes.

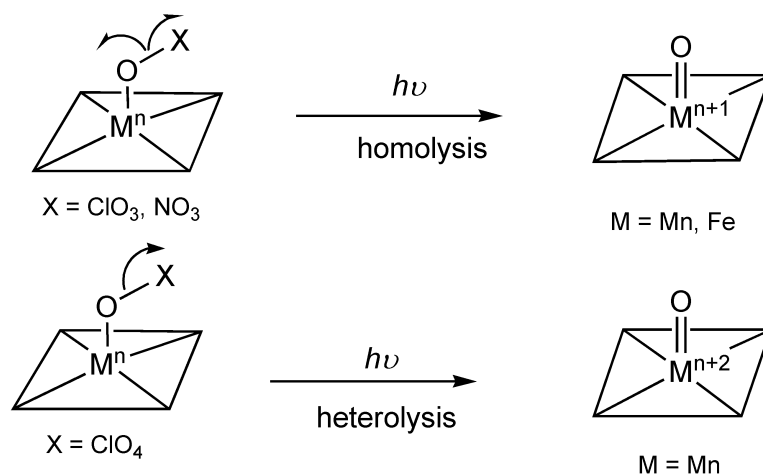
Ruthenium porphyrin complexes are among the most extensively studied biomimetic catalysts for hydrocarbon oxidation because of their rich coordination and redox chemistry.<sup>1,17,21,54</sup> In particular, *trans*-dioxoruthenium(VI) porphyrin complexes (**6**), abbreviated as Ru<sup>VI</sup>(Por)(O)<sub>2</sub>, have received considerable attention as model systems for heme-containing enzymes.<sup>54-56</sup> This interesting family of ruthenium complexes exhibits significant reactivity toward organic substrates, such as phosphines, sulfides, alcohols and hydrocarbons.<sup>57-59</sup> Notably, *trans*-dioxoruthenium(VI) porphyrins have been

shown to catalyze the clean aerobic epoxidation of olefins in the absence of a reducing agent under mild conditions.<sup>60</sup> Although *trans*-dioxoruthenium(VI) derivatives are the best characterized oxidizing intermediates, their involvement as the active oxidant in the catalytic cycle of ruthenium porphyrins with aromatic *N*-oxides as the oxygen source has been ruled out in view of the low reactivity and enantioselectivity.<sup>61,62</sup>

The first isolation and characterization of the sterically hindered *trans*-dioxoruthenium(VI) porphyrin complex, Ru<sup>VI</sup>(TMP)(O)<sub>2</sub> (TMP = 5,10,15,20-tetramesityporphyrinato dianion) by oxidation of Ru<sup>II</sup>(TMP)(CO) with meta-chloroperoxybenzoic acid (*m*-CPBA) was reported by Groves and Quinn.<sup>63</sup> Che and co-workers had reported the syntheses of non-sterically encumbered *trans*-dioxoruthenium(VI) porphyrins Ru<sup>VI</sup>(TPP)(O)<sub>2</sub> (TPP = 5,10,15,20-tetraphenylporphyrinato dianion) and Ru<sup>VI</sup>(OEP)(O)<sub>2</sub> (OEP = octaethylporphyrinato dianion) in the presence of coordinating solvents (such as methanol).<sup>64</sup> The choice of solvent is very important to the success of the synthesis, presumably due to the coordination of alcohol on the ruthenium(IV) intermediate, which can inhibit the formation of  $\mu$ -oxo dimer. In addition to peroxyacids, other sacrificial oxidants, such as iodosylbenzene (PhIO), periodate, and *tert*-butyl hydroperoxide (TBHP) were able to produce the *trans*-dioxoruthenium(VI) species.<sup>17,63</sup> Later, chiral *trans*-dioxoruthenium(VI) complexes were prepared in similar manners and characterized with satisfactory spectroscopic properties.<sup>62,65,66</sup> Some *trans*-dioxoruthenium(IV) porphyrin complexes are even determined by X-ray crystal structures.<sup>56,67</sup>

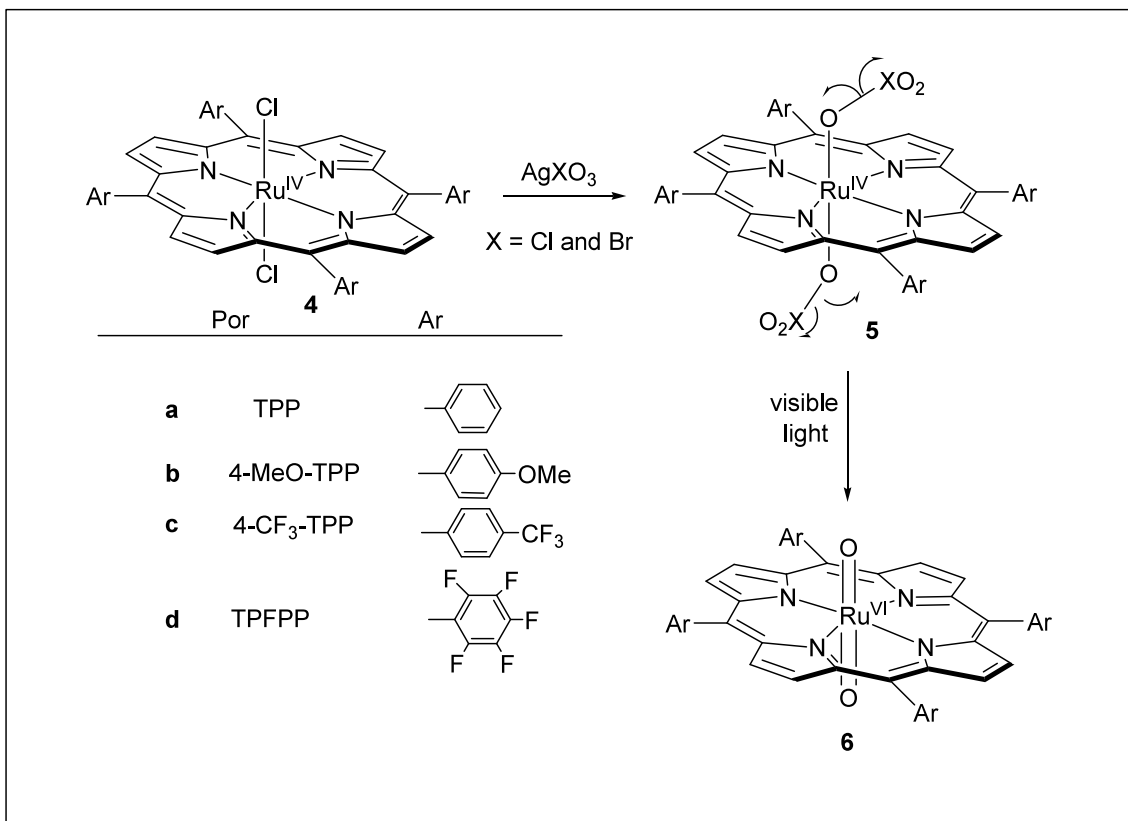
Our particular interest in the context of metal-oxo chemistry is to explore the photochemical approach that targets the direct detection and kinetic study of high-valent

transition metal-oxo derivatives. With photochemical production of reactive metal-oxo transients, one has access to time scales that are much shorter than the fastest mixing experiments and kinetics of oxidation reactions of the transients of interest are not convoluted with the kinetics of reactions that form the transients. Recently, photo-induced ligand cleavage reactions have been developed to generate a variety of metal-oxo species.<sup>68-70</sup> The concept of photo-induced ligand cleavage reactions is very straightforward, as illustrated in Scheme 11. The precursors are metal complexes with the metal in the  $n$  oxidation state and an oxygen-containing ligand such as perchlorate, chlorate, or nitrate. Photolysis can result in homolytic cleavage of the O–X bond in the ligand to give an  $(n + 1)$  oxidation state metal-oxo species (one electron photo-oxidation) or heterolytic cleavage of the O–X bond in the ligand to give an  $(n + 2)$  oxidation state metal-oxo species (two electron photo-oxidation). Although straightforward in concept, the creation of photochemical methods for formation of metal-oxo species requires considerable development of the requisite photochemical methods and especially the photo-labile precursors. For example, photochemical cleavages of porphyrin-manganese(III) nitrates or chlorates, corrole-manganese(IV) chlorates, and corrole-iron(IV) chlorates, give neutral porphyrin-manganese(IV)-oxo, corrole-manganese(V)-oxo, and corrole-iron(V)-oxo derivatives, respectively, by homolytic cleavage of the O–Cl or O–N bond in the axial ligand. On the other hand, photolysis of porphyrin-manganese(III) perchlorate complexes gave much more reactive porphyrin-manganese(V)-oxo transients by heterolytic cleavage of the O–Cl bond in perchlorate.



**Scheme 11.** Generation of high-valent metal-oxo species by photo-induced ligand cleavage reactions.

The photo-induced ligand cleavage reactions has been extended to produce the well-known *trans*-dioxoruthenium(VI) complexes by irradiation of porphyrin–ruthenium(IV) dichlorate complexes with visible light (Scheme 12).<sup>71</sup> This photochemical method can efficiently generate the *trans*-dioxoruthenium(VI) complexes in sterically bulky and non-bulky porphyrins without the limitation of porphyrin ligands as observed in chemical methods.<sup>71</sup> In this chapter we describe our full findings on the photochemical generation of *trans*-dioxoruthenium(VI) complexes are described by irradiation of porphyrin–ruthenium(IV) dichlorate or dibromate complexes that result in homolytic cleavage of the O–X bond in both axial ligands Scheme 12. This photochemical method can be used to generate the *trans*-dioxoruthenium(VI) in various porphyrin systems under similar condition, in particular the very electron-demanding  $\text{Ru}^{\text{VI}}(\text{TPFPP})\text{O}_2$  (TPFPP = tetrakis(pentafluorophenyl)porphyrinatodianion).



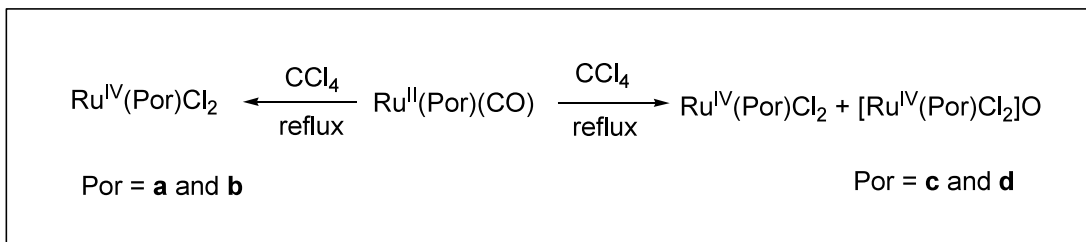
**Scheme 12.** Photochemical generation of *trans*-dioxoruthenium(VI) porphyrins.

The porphyrin systems studied are shown in Scheme 12, using abbreviations that follow those conventionally established. The different aromatic groups on the porphyrins also result in varying electron demands with the phenyl system being least electron withdrawing, the 4-methoxyphenyl system (**b**), and the pentafluorophenyl system (**d**) are the most electron withdrawing.

#### 4.2. Preparation of dichlororuthenium(IV) porphyrin $[\text{Ru}^{\text{IV}}(\text{Por})\text{Cl}_2]$ **4**

The study started with the preparation of dichlororuthenium(IV) porphyrins,  $\text{Ru}^{\text{IV}}(\text{Por})\text{Cl}_2$  (**4**), that can be readily prepared by heating the carbonyl precursor  $\text{Ru}^{\text{II}}(\text{Por})(\text{CO})$  (**2**) in  $\text{CCl}_4$  in air as described by Gross and Barzilay (Scheme 13).<sup>72</sup> The oxidative transformation is characterized by a distinct color change from orange red to dark brown, accompanied by the blue-shift of the Soret bands ( $\text{CHCl}_3$ ). Interestingly,  $\text{Ru}^{\text{II}}(\text{Por})(\text{CO})$  with sterically unhindered ligands (Por = TPP (**a**) and 4-MeO-TPP (**b**)) also gave the desired products **4a** and **4b** predominately. However, the same procedure for the sterically unhindered porphyrins with electron-withdrawing substituents (Por = 4- $\text{CF}_3$ -TPP (**c**) and TPFPP (**d**)) led to the formation of substantial amounts of  $\mu$ -oxo dimer by products,  $[\text{Ru}^{\text{IV}}(\text{Por})\text{Cl}]_2\text{O}$ , along with  $\text{Ru}^{\text{IV}}(\text{Por})\text{Cl}_2$  (**4c** and **4d**). The former by products were identified by its diamagnetic  $^1\text{H}$  NMR signals similar to those of  $[\text{Ru}^{\text{IV}}(\text{TPP})\text{Cl}]_2\text{O}$ .<sup>41</sup> Using an alternative method by reacting the corresponding  $\text{Ru}^{\text{VI}}(\text{Por})(\text{O})_2$  with  $\text{Me}_3\text{SiCl}$  or  $\text{HCl}$  gave a similar result.<sup>73</sup> The reason for the marked dependence of formation of  $\mu$ -oxo dimer on the porphyrin substituents is not yet clear. It seems that electron-withdrawing substituents, such as  $\text{CF}_3$  and F, on porphyrin ligand favor  $\mu$ -oxo dimer formation. Presumably, the electron-withdrawing substituents would stabilize the ruthenium(IV) complex in a dimer form by reducing the electron density of metal atoms. We also found the amount of  $\mu$ -oxo dimer was highly dependent on the reaction concentration, i.e. refluxing the carbonyl ruthenium(II) precursors in higher concentration in  $\text{CCl}_4$  gave a less amount of  $\mu$ -oxo dimers. The origin of the considerable effect of substituent and concentration on the formation of  $\mu$ -oxo dimer is not apparent, and this subject deserves further study. Following a known procedure,<sup>74</sup> complexes **4c**

and **4d** with electron-deficient sterically unhindered porphyrin were purified by refluxing the crude mixtures in a Soxhlet apparatus with diethyl ether to remove the  $\mu$ -oxo dimer by products.



**Scheme 13.** Synthesis of dichlororuthenium(IV) porphyrins complexes **4**

In a typical run,  $\text{Ru}^{\text{IV}}(\text{Por})\text{Cl}_2$  (**4**) was prepared by refluxing  $\text{Ru}^{\text{II}}(\text{Por})(\text{CO})$  (**2**) complexes (50 mg) in  $\text{CCl}_4$  (30 mL) and monitored by UV-vis spectroscopy. The refluxing time, ranging from 2 h to overnight, depended on the porphyrin system employed. The  $\text{Ru}^{\text{IV}}(\text{Por})\text{Cl}_2$  (**4c** and **4d**) with electron-deficient sterically unhindered porphyrin (4- $\text{CF}_3$ -TPP and TPFPP) were readily purified by refluxing the crude mixture in a Soxhlet apparatus with diethyl ether to remove the  $\mu$ -oxo dimer by products.

$[\text{Ru}^{\text{IV}}(\text{TPP})\text{Cl}_2]$  (**4a**). Yield = 95%.  $^1\text{H}$  NMR (500 MHz,  $\text{CDCl}_3$ )  $\delta$ , ppm: -58.2 (s, 8H,  $\beta$ -pyrrole). UV-vis ( $\text{CH}_3\text{CN}$ )  $\lambda_{\text{max}}/\text{nm}$ : 408 (Soret), 528.

$[\text{Ru}^{\text{IV}}(4\text{-MeO-TPP})\text{Cl}_2]$  (**4b**). Yield = 86%.  $^1\text{H}$  NMR (500 MHz,  $\text{CDCl}_3$ )  $\delta$ , ppm: -53.8 (s, 8H,  $\beta$ -pyrrole). UV-vis ( $\text{CH}_3\text{CN}$ )  $\lambda_{\text{max}}/\text{nm}$ : 406 (Soret), 525.

$[\text{Ru}^{\text{IV}}(4\text{-CF}_3\text{-TPP})\text{Cl}_2]$  (**4c**). Yield = 43%.  $^1\text{H}$  NMR (500 MHz,  $\text{CDCl}_3$ )  $\delta$ , ppm: -57.6 (s, 8H,  $\beta$ -pyrrole). UV-vis ( $\text{CH}_3\text{CN}$ )  $\lambda_{\text{max}}/\text{nm}$ : 406 (Soret), 530.

$[\text{Ru}^{\text{IV}}(\text{TPFPP})\text{Cl}_2]$  (**4d**). Yield = 48%.  $^1\text{H}$  NMR (500 MHz,  $\text{CDCl}_3$ )  $\delta$ , ppm: -53.3 (s, 8H,  $\beta$ -pyrrole). UV-vis ( $\text{CH}_3\text{CN}$ )  $\lambda_{\text{max}}/\text{nm}$ : 405 (Soret), 525.



#### 4.3. Preparation of porphyrin- ruthenium(IV) dichlorates $[\text{Ru}^{\text{IV}}(\text{Por})(\text{ClO}_3)_2]$ **5**

Each of the dichlororuthenium(IV) complexes were characterized by its distinct paramagnetically shifted pyrrolic protons (Figure 12B) ( $\delta$  ranging from -52.3 to -58.2 ppm).<sup>72</sup> Facile exchange of the counterions in **4** with  $\text{Ag}(\text{ClO}_3)$  gave the corresponding dichlorate salts **5** that were characterized by UV–Vis and  $^1\text{H}$  NMR spectra. Complexes **5** are photo-labile and can be handled for a short time in solutions exposed to light. Interestingly, ruthenium(IV) dichlorate complexes **5** show UV–vis (figure 12A) and paramagnetic  $^1\text{H}$  NMR spectra, similar to those of dichloro compounds **4**. In the  $^1\text{H}$  NMR spectra of **4** and **5**, the paramagnetic pyrrolic signal of **5** is located at -20 ppm, slightly more downfield than that of paramagnetic **4**, consistent with weaker binding ability of chlorate than that of chloride. The distinct pyrrolic shift is shown in (figure 12B).

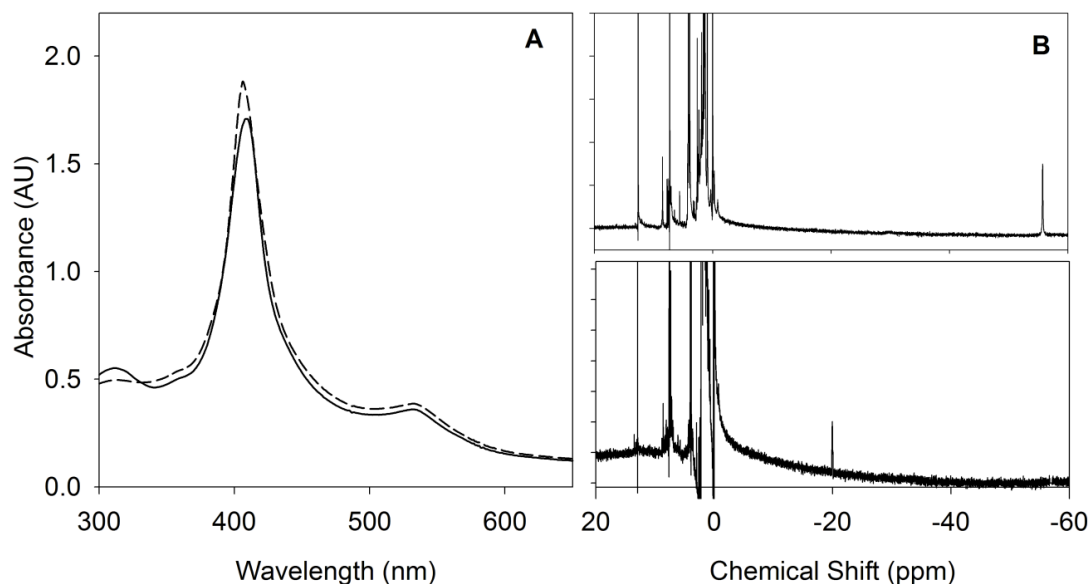


**Figure 12.** (A) Typical UV-Vis spectra of  $\text{Ru}^{\text{IV}}(\text{TPP})\text{Cl}_2$  **4a**, (dashed) and  $\text{Ru}^{\text{IV}}(\text{TPP})(\text{ClO}_3)_2$  **5a**, (solid) in  $\text{CH}_3\text{CN}$ . (B)  $^1\text{H}$  NMR spectrum of  $\text{Ru}^{\text{IV}}(\text{TPP})\text{Cl}_2$  **4a**, (top) and  $\text{Ru}^{\text{IV}}(\text{TPP})(\text{ClO}_3)_2$  **5a**, (bottom) in  $\text{CDCl}_3$ .

#### 4.4. Photolysis of porphyrin–ruthenium(IV) dichlorates $[\text{Ru}^{\text{IV}}(\text{Por})(\text{ClO}_3)_2]$ (**5**)

Irradiation of chlorate complexes **5** in anaerobic  $\text{CH}_3\text{CN}$  with visible light from a tungsten lamp (100 W) resulted in homolytic cleavage of the O–Cl bond in the two chlorate counterions to produce neutral dioxoruthenium(VI) species (**6**). Figure 13 shows representative time-resolved formation spectra of  $\text{Ru}^{\text{VI}}(\text{Por})(\text{O})_2$  in two different porphyrin systems, i.e., non-sterically hindered (**6a**) and electron-efficient (**6d**). These time-resolved UV–Vis spectra show decay of photo-labile precursors (**5**) and growth of the products (**6**) in absorption spectra with clean isosbestic points. In each case, the formed species **6** display a stronger red-shifted Soret and a blue-shifted weaker Q bands that are characteristic for the corresponding *trans*-dioxoruthenium(VI) porphyrins.<sup>63,64</sup> This general approach is applicable to the evidently most reactive **6d** bearing the most electron demanding porphyrin (TPFPP).<sup>61</sup> The formation of **6d** by photochemical oxidation was also observed with a slowest rate among all systems studied Figure. 13B; this is in line with the expected highest oxidation potential of the  $\text{Ru}^{\text{IV}}$  species **4d** with the most electron-withdrawing porphyrin ring of TPFPP.<sup>56</sup> The identities of complexes **6** as  $\text{Ru}^{\text{VI}}(\text{Por})(\text{O})_2$  generated in photochemical reactions were further confirmed by UV–Vis and  $^1\text{H}$ -NMR.

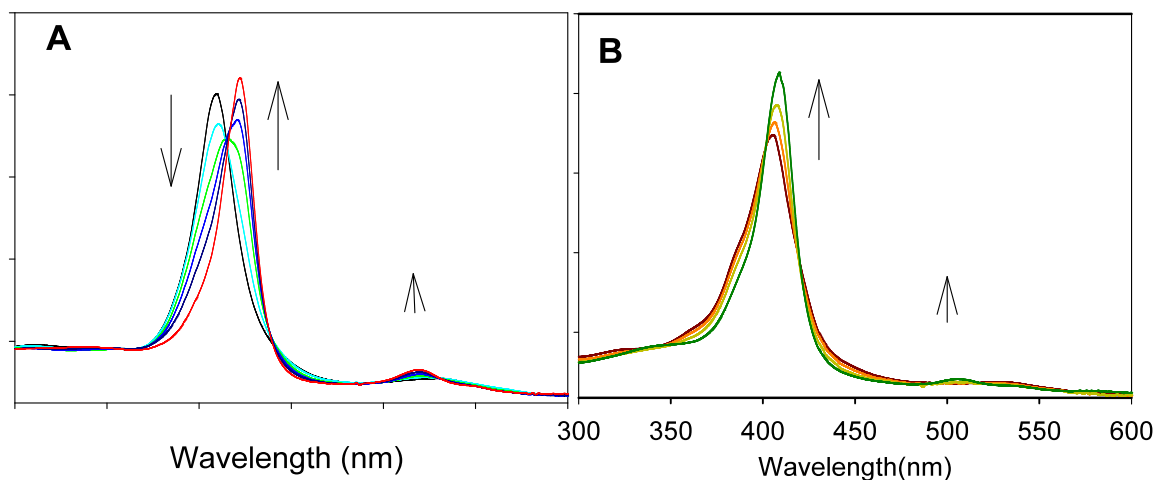


**Figure. 13** Examples of generation of *trans*-dioxoruthenium(VI) species (**6**) by photolysis of the corresponding dichlorate precursors (**5**). In these time-resolved difference spectra, species (**5**) are decaying away with time, and species (**6**) with red-shifted Soret absorbance are growing in with time. (A) Spectrum of Ru<sup>VI</sup>(TPP)(O)<sub>2</sub> (**5a**) following photolysis of chlorate salt (**5a**) in CH<sub>3</sub>CN over a total time of 45 min. (B) Spectrum of Ru<sup>VI</sup>(TPFPP)(O)<sub>2</sub> (**6d**) following photolysis of chlorate salt (**5d**) in CH<sub>3</sub>CN over a total time of 160 min.

Control experiments showed that no dioxo species was formed in the absence of light. As expected, using more intensive light (max = 420 nm, ca. 300 W) resulted in faster formation of **6** in the same solvent. The use of other non-coordinating solvents, such as CH<sub>2</sub>Cl<sub>2</sub> or THF, also gave similar results. However, no reaction was observed when methanol or ethanol was used. Presumably, the weakly binding chlorate counterions were displaced by these coordinating solvents.

It is noteworthy that the photochemical reactions of chlorates **5** appears to present a reaction manifold similar to that of porphyrinmanganese(III) chlorates,<sup>48</sup> corrole-manganese(IV) chlorates<sup>36</sup> and corrole-iron(IV) chlorates,<sup>38</sup> which result in homolytic cleavage of the O–Cl bond in the chlorate. Photolysis of  $\text{Mn}^{\text{III}}(\text{Por})(\text{NO}_3)$  complexes was reported to give  $\text{Mn}^{\text{IV}}(\text{Por})(\text{O})$  species by homolytic cleavage of an O–N bond,<sup>68</sup> similar to those of chlorate complexes albeit with considerably less efficiency.<sup>48</sup> However, we found that photolysis of dinitrate ruthenium(IV) complexes did not afford the dioxo complexes **6** even with prolonged irradiation and higher-energy light (max = 350 nm). The reaction generated an unknown product with slightly blue-shifted Soret band (data not shown). We did not observe any photochemical reactions when we irradiated the ruthenium(IV) diperchlorates, i.e.  $\text{Ru}^{\text{VI}}(\text{Por})(\text{ClO}_4)_2$  under similar conditions.

#### 4.4.1 Photolysis of porphyrin–ruthenium(IV) dibromates $[\text{Ru}^{\text{IV}}(\text{Por})(\text{BrO}_3)_2]$

Photolysis of  $\text{Ru}^{\text{IV}}(\text{Por})(\text{BrO}_3)_2$  complexes producing dioxoruthenium(VI) species also were possible. The photolabile ruthenium(IV) dibromates were produced *in situ* from the chlorides (**4**) by counterion exchange with  $\text{AgBrO}_3$ . Irradiation of resulting dibromate species with visible light gave *trans*-dioxoruthenium(VI) porphyrin with well-anchored isosbestic points Figure 14. The photochemical reaction that gave homolytic cleavage of the O–Br bonds is directly the same as that of the ruthenium(IV) chlorates.

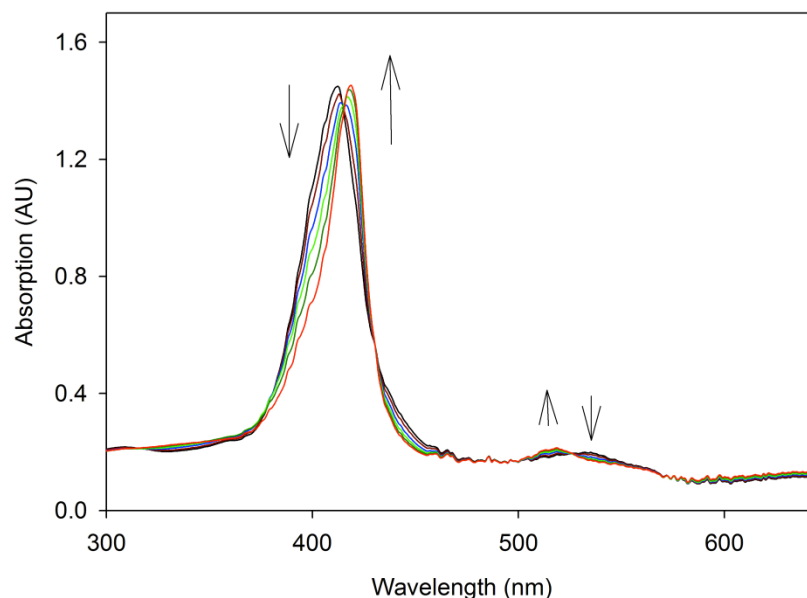


**Figure. 14.** UV–Vis spectral change of **1a** ( $8 \times 10^{-6}$  M) with 5-fold excess of  $\text{AgBrO}_3$  in anaerobic  $\text{CH}_3\text{CN}$  solution upon irradiation with a 100W tungsten lamp at  $22^\circ\text{C}$  over 80 min.

#### 4.5. Generation procedure for photosynthesis of *trans*-dioxoruthenium(VI) porphyrins $[\text{Ru}^{\text{VI}}(\text{Por})(\text{O})_2]$ (**6**)

Treatment of compounds **4** (ca. 10 mg) with 2–5 folds excess of  $\text{AgClO}_3$  in  $\text{CH}_3\text{CN}$  gave the dichlorate **5** complexes that were generated *in situ* in most runs, and directly used in subsequent photochemical reactions immediately after preparation. When the solution of **5** at desired concentration ( $\sim 1 \times 10^{-5}$  M) was irradiated with a 100W of visible light from a tungsten lamp at ambient temperature, the formation of **6** was complete in ca. 50 min, as monitored by UV–Vis spectroscopy. The dioxo complexes **6** were isolated as dark red–purple crystalline solids, and can be readily purified by passing through a short dry column (basic alumina) to give satisfactory spectroscopic characterization spectra.

[Ru<sup>VI</sup>(TPP)(O)<sub>2</sub>] (**6a**): Yield = 86%. <sup>1</sup>H NMR (500 MHz, CDCl<sub>3</sub>): δ 9.1 (s, 8H), 8.6 (d, 8H), 8.4 (d, 4H), 7.8 (m, 8H). UV–Vis (CH<sub>2</sub>Cl<sub>2</sub>) λ max/nm: 420 (Soret band), 520 (Q band).

[Ru<sup>VI</sup>(4-MeOTPP)(O)<sub>2</sub>] (**6b**): Yield = 94%. <sup>1</sup>H NMR (500 MHz, CDCl<sub>3</sub>): δ 9.1 (s, 8H), 8.2 (d, 8H), 7.3 (d, 8H), 4.2 (s, 12H). UV–Vis (CHCl<sub>3</sub>) λ max/nm: 425 (Soret band), 525 (Q band), 550 (sh).

[Ru<sup>VI</sup>(4-CF<sub>3</sub>TPP)(O)<sub>2</sub>] (**6c**): Yield = 89%. <sup>1</sup>H NMR (500 MHz, CDCl<sub>3</sub>): δ 9.0 (s, 8H), 8.5 (d, 8H), 8.1 (d, 8H). UV–Vis (CHCl<sub>3</sub>) λ max/nm: 418 (Soret band), 520 (Q band).

[Ru<sup>VI</sup>(TPFPP)(O)<sub>2</sub>] (**6d**): Yield = 82%. <sup>1</sup>H NMR (300 MHz, CDCl<sub>3</sub>): δ, ppm: 9.18 (s, 8H). UV–Vis (CH<sub>2</sub>Cl<sub>2</sub>) λ max/nm: 412 (Soret), 506

## V. CONCLUSIONS

The *trans*-dioxoruthenium(VI) porphyrins have been among the best characterized metal-oxo intermediates, and their involvement as the active oxidant in the alkene epoxidations and alkane hydroxylation have been extensively studied. A new photochemical approach to prepare *trans*-dioxoruthenium(VI) porphyrin complexes is discovered by photolysis of the corresponding ruthenium(IV) dichlorates or dibromates with visible light. With this method a variety of *trans*-dioxoruthenium(VI) porphyrins are produced without the limitation of porphyrin ligands. This work also demonstrates, for the first time, that a two electron photo-oxidation can be achieved by two simultaneous homolytic bond cleavages, i.e. two one-electron photooxidation. Given that porphyrin–ruthenium(V)-oxo transients are more attractive candidates for oxidations,<sup>61,74,75</sup> the extension of this method for generation of the elusive ruthenium(V)-oxo species is underway in our laboratory.

The photocatalytic aerobic oxidation of hydrocarbons by the ruthenium(IV)  $\mu$ -oxo bisporphyrin complexes using visible light and atmospheric oxygen as oxygen source was investigated. The ruthenium(IV)  $\mu$ -oxo bisporphyrin **6c** was found to catalyze aerobic oxidation of a variety of organic substrates efficiently. Significant activity was observed with TONs up to 3900. For comparison, the photocatalytic aerobic epoxidation of *cis*-cyclooctene by **3c** was also conducted under the identical conditions. Obviously, **3c** was a more efficient photocatalyst than the well-known **6a**. Competitive catalytic oxidation of ethylbenzene and ethylbenzene-*d*<sub>10</sub> revealed a larger KIE value at 298K than those observed in autoxidation processes, suggesting a nonradical mechanism that involved the intermediacy of ruthenium(V)-oxo species as postulated.

## REFERENCES

1. Sheldon, R.A.; Dekker, M. "Metalloprophyrins in Catalytic Oxidations" *New York*, **1994**.
2. Punniyamurthy, T.; Velusamy, S.; Iqbal. "Recent Advances in Transition Metal Catalyzed Oxidation of Organic Substrates with Molecular Oxygen" *J. Chem. Rev.* **2005**, *105*, 2329–2363.
3. Backwell, J.-E.; Piera J. "Catalytic oxidation of organic substrates by molecularoxygen and hydrogen peroxide by multistep electron transfer – A biomimetic approach." *Angew. Chem. Int. Ed.* **2008**, *47*, 3506 – 3523.
4. Brink, G.-J.; Arends, I.W.C.E.; Sheldon, R.A. "Green catalytic oxidation of alcohols in water." *Science*, **2000**, *287*, 1636 – 1639.
5. Zhang, R. Asymmetric organic oxidation by chiral ruthenium complexes containing D<sub>2</sub> – and D<sub>4</sub> symmetric porphyrinato ligands. *Ph. D. Thesis* **2000**, 1 – 235.
6. Denisov, L.-G.; Makris, M.-T.; Sligar, G.-S.; Schlichting, L. "Structure and chemistry of cytochrome P450." *Chem. Rev.* **2005**, *105*, 2253 – 2277.
7. Newcomb, M.; Zhang, R.; Chandrasena, E. P.; Halgrimson, J. A.; Horner, J. H.; Makris, M. T.; Sligar, S. G. "Cytochrome P450 Compound I." *J. Am. Chem. Soc.* **2006**, *128*, 4580 – 4581.
8. Masanori, S.; Roach, M. P.; Coulter, E. D.; Dawson, J. H. "Heme – Containing Oxygenases." *Chem. Rev.* **1996**, *96*, 2841 – 2887.



9. Rui, L.; Pochapsky, S. S.; Pochapsky, C. T. "Comparison of the complexes formed by cytochrome P450<sub>cam</sub> with cytochrome b<sub>5</sub> and putidaredoxin, two effectors of camphor hydroxylase activity". *Biochem.* **2006**, *45*, 3887 – 3897.
10. Meunier, B. "Metal-oxo and metal-peroxo species in catalytic oxidations." *Academic Press: New York*, **2000**.
11. Zhang, R.; Nagraj, N.; Lansakara-P., D.S.P.; Hager, L.-P.; Newcomb, M. "Kinetics of two-electron oxidation by the Compound I derivative of chloroperoxidase, a model for cytochrome P450 oxidants." *Org. Lett.* **2006**, *8*, 2731 – 2734.
12. Groves, J.-T. "Reactivity and mechanism of metalloporphyrin-catalyzed oxidations." *J. Porph. Phthal.* **2000**, *4*, 350 – 352.
13. Sheldon, R, Kochi J. "Metal-catalyzed oxidations of organic compounds." *Academic Press: New York*, **1981**.
14. Simandi, L. "Dioxygen activation and homogeneous catalytic oxidation." *Elsevier: Amsterdam*, **1991**.
15. Wang, C.; Shalyaev, K.V.; Bonchio, M.; Carofiglio, T.; Groves, J.T. "Fast catalytic hydroxylation of hydrocarbons with ruthenium porphyrins." *Inorg. Chem.* **2006**, *45*, 4769 – 4782.
16. Che, C.-M.; Zhang, R.; Yu, W.-Y. "Catalytic enantioselective oxidation of aromatic hydrocarbons with D<sub>4</sub>-symmetric chiral ruthenium porphyrin catalysts." *Tetrahedron: Asymmetry* **2005**, *16*, 3520 – 3526.
17. Groves, J.T.; Shallyaev, K.; Lee, J. "The Porphyrin Handbook" **2000**, *4*, 17 – 40.
18. Collins, T.; Oliveira, F.; Chanda, A.; Banerjee, D.; Shan, X.; Mondal, S.

- “Chemical and Spectroscopic Evidence for an FeV-Oxo Complex.” *Science*. **2007**, 315, 835 –838.
19. Davies, J. “Selective hydrocarbon activation: Principle and progress.” *VCH: New York*, **1994**.
  20. Che, C.-M.; Leung, W.-H. “High-Valent Ruthenium(IV) and –(VI) oxo complexes of octaethylporphyrin. Synthesis, spectroscopy, and reactivities.” *J. Am. Chem. Soc.* **1989**, 111, 8812 – 8818.
  21. Meunier B. “Metalloporphyrins as versatile catalysts for oxidation reactions and oxidative DNA cleavage.” *Chem. Rev.* **1992**, 92, 1411 – 1456.
  22. Groves, J.T.; Lee, J.; Marla, S.S. “Detection and characterization of an oxomanganese(V) porphyrin complex by rapid-mixing stopped-flow spectrophotometry.” *J. Am. Chem. Soc.*, **1997**, 119, 6269 – 6273.
  23. Huang, Y.; Vanover, E.; Zhang, R. “A facile photosynthesis of transdioxoruthenium(VI) porphyrins.” *Chem. Commun.*, **2010**, 46, 3776 – 3778.
  24. Albini, A. *J. Chem. Educ.* **1986**, 63, 383.
  25. Hennig, H.; Billing, R.; Knoll, H. “In Photosensitization and Photocatalysis Using Inorganic and Organometallic Compounds”. Kalyanasundaram, K., Gratzel, M., Eds.; *Kluwer Academic Publishers: Dordrecht, The Netherlands*, **1993**; 51.
  26. Kisch, H. Serpone, N., Pelizzetti, E., Eds “In Photocatalysis-Fundamentals and Application”. *Wiley-Interscience: New York*, **1989**; 1.
  27. Maldotti, A. Molinari, A. Amadelli, R. “Photocatalysis with Organized Systems for the Oxofunctionalization of Hydrocarbons by O<sub>2</sub>” *Chem. Rev.* **2002**, 102, 3811-3836.

28. Hamilton, G.A.; Hayaishi, O “In molecular mechanisms of oxygen activation; Ed.” *Academic: New York*, **1974**, *10*, 405 – 451.
29. Ullrich, V. “Topics in current chemistry.” **1979**, *83*: 67.
30. Vanover, E.; Huang, Y.; Xu, L.-B.; Newcomb, M.; Zhang, R. “Photocatalytic aerobic oxidation by a bis-porphyrin-ruthenium(VI)  $\mu$ -oxo dimer: observation of a putative porphyrin-ruthenium(V)-oxo intermediate.” *Org. Lett.* **2010**, *12*, 2246 - 2249.
31. Che, C.-M.; Huang, J.-S. “Metalloporphyrin-based oxidation systems: From biomimetic reactions to application in organic synthesis.” *Chem. Commun.* **2009**, *55*, 3996-4015.
32. Bäckvall, J. E. “Modern oxidation methods”. Wiley-VCH Verlag: Weinheim, **2004**.
33. Punniyamurthy, T.; Velusamy, S.; Iqbal, J. “Recent advances in transition metal catalyzed oxidation of organic substrates with molecular oxygen.” *Chem. Rev.*, **2005**, *105*, 2329 – 2364.
34. Peterson, M.W.; Rivers, D.S.; Richman, R.M. “Mechanistic considerations in the photodisproportionation of  $\mu$ -oxo-bis((tetraphenylporphinato)iron(III)).” *J. Am. Chem. Soc.*, **1985**, *107*, 2907–2915.
35. Tiago de Oliveira, F.; Chanda, A.; Banerjee, D.; Shan, X.; Mondal, S.; Que, L., Jr.; Bominaar, E. L.; Muenck, E.; Collins, T. J. “Chemical and Spectroscopic Evidence for an FeV-Oxo Complex.” *Science* **2007**, *315*, 835–838.
36. Harischandra, D. N.; Zhang, R.; Newcomb, M. J. “Photochemical Generation of a Highly Reactive Iron-Oxo Intermediate. A True Iron(V)-Oxo Species?” *Am.*

- Chem. Soc.* **2005**, *127*, 13776–13777.
37. Pan, Z.; Zhang, R.; Fung, L. W. M.; Newcomb, M. “Photochemical Production of a Highly Reactive Porphyrin-Iron-Oxo Species.” *Inorg. Chem.* **2007**, *46*, 1517–1519.
  38. Harischandra, D. N.; Lowery, G.; Zhang, R.; Newcomb, M. “Production of a Putative Iron(V)-Oxo Corrole Species by Photo-Disproportionation of a Bis-Corrole-Diiron(IV)-  $\mu$ -Oxo Dimer: Implication for a Green Oxidation Catalyst.” *Org. Lett.* **2009**, *11*, 2089–2092.
  39. Adler, A.D.; Longo, F.R.; Finarelli, J.D.; Goldmacher, J.; Assour, J.; Korsakoff, L. “A Simplified synthesis for *meso*-Tetraphenylporphin”. *J. Org. Chem.* **1966**, *32*, 476.
  40. Che, C.-M.; Zhang, J.-L.; Zhang, R.; Huang, J.-S.; Lai, T.-S.; Tsui, W.-M, Zhou, X.-G.; Zhou, Z.-Y.; Zhu, N.; Chang, C. K. “Hydrocarbon oxidation by  $\beta$ -halogenated dioxoruthenium(VI) porphyrin complexes: Effect of reduction potential ( $\text{Ru}^{\text{VI/V}}$ ) and C – H bond-dissociation energy on rate constants.” *Chem. Eur. J.* **2005**, *11*, 7040 – 7053.
  41. Sugimoto, H.; Higashi, T.; Mori, M.; Nagano, M.; Yoshida, Z.-I.; Ogoshi, H. “Preparation and physicochemical properties of new linear  $\mu$ -oxo bridged ruthenium(IV) and osmium(IV) porphyrin dimers.” *Bull. Chem. Soc. Jpn.* **1982**, *55*, 822 – 828.
  42. Collman, J. P.; Barnes, C. E.; Brothers, P. J.; Collins, T. J.; Ozawa, T.; Gallucci, J. C.; Ibers, J. A. “Oxidation of ruthenium(II) and ruthenium(III) porphyrins. Crystal structures of  $\mu$ -oxo-bis[(*p*-methylphenoxo)(*meso*-tetraphenylporphyrinato)ruthenium(IV)] and ethoxo(*meso*-

- tetraphenylporphyrinato)(ethanol)ruthenium(III)-bisethanol.” *J. Am. Chem. Soc.* **1984**, *106*, 5151–5163.
43. Kearns, D. R. “Physical and Chemical Properties of Singlet Molecular Oxygen.” *Chem. Rev.* **1971**, *71*, 395–427.
44. Pan, Z.; Zhang, R.; Newcomb, M. J. “Kinetic studies of reactions of iron(IV)-oxo porphyrin radical cations with organic reductants.” *Inorg. Biochem.* **2006**, *100*, 524–532.
45. Sawyer, D. T.; Kang, C.; Llobet, A.; Redman, C. “Fenton reagents (1:1 FeII/Lx/HOOH) react via [LxFeIIOOH(BH<sup>+</sup>)] (1) as hydroxylases (RH → ROH), not as generators of free hydroxyl radicals (HO•).” *J. Am. Chem. Soc.* **1993**, *115*, 5817–5818.
46. Meunier, B. “Metal-Oxo and Metal-Peroxo Species in Catalytic Oxidations” *Springer-Verlag, Berlin*, **2000**.
47. Costas, M.; Mehn, M.P.; Jensen, L. Que. “Dioxygen Activation at Mononuclear Nonheme Iron Active Sites: Enzymes, Models, and Intermediates.” *Chem. Rev.* **2004**, *104* (2004) 939.
48. Zhang, R.; Horner, J.H.; Newcomb, M. “Laser Flash Photolysis Generation and Kinetic Studies of Porphyrin-Manganese-Oxo Intermediates. Rate Constants for Oxidations Effected by Porphyrin-MnV-Oxo Species and Apparent Disproportionation Equilibrium Constants for Porphyrin-MnIV-Oxo Species.” *J. Am. Chem. Soc.* **2005**, *127*, 6573.
49. Collman, J.P.; Chien, A.S.; Eberspacher, T.A.; Brauman, J.I. “Multiple Active Oxidants in Cytochrome P-450 Model Oxidations.” *J. Am. Chem. Soc.*

- 2000**, *122*, 11098-11100.
50. Nam, W.; Lim, M.H.; Lee, H.J.; Kim, C. "Evidence for the Participation of Two Distinct Reactive Intermediates in Iron(III) Porphyrin Complex-Catalyzed Epoxidation Reactions." *J. Am. Chem. Soc.* **2000**, *122*, 6641-6647.
51. Nam, W.; Lim, M.H.; Moon, S.K.; Kim, C. "Participation of Two Distinct Hydroxylating Intermediates in Iron(III) Porphyrin Complex-Catalyzed Hydroxylation of Alkanes." *J. Am. Chem. Soc.* **2000**, *122*, 10805.
52. Newcomb, M.; Shen, R.; Choi, S.; Toy, P.H.; Hollenberg, P.F.; Vaz, A.D.N.; Coon, M.J. "Cytochrome P450-Catalyzed Hydroxylation of Mechanistic Probes that Distinguish between Radicals and Cations. Evidence for Cationic but Not for Radical Intermediates." *J. Am. Chem. Soc.* **2000**, *122*, 2677.
53. Che, C.-M.; Huang, J.-S. "Metalloporphyrin-based oxidation systems: from bioimetic reactions to application in organic synthesis." *Chem. Commun.* **2009**, 3996.
54. Che, C.-M.; Yu, W.-Y. "Ruthenium-oxo and -tosylimido porphyrin complexes for epoxidation and aziridination of alkenes." *Pure Appl. Chem.* **1999**, *71*, 281.
55. Zhang, R.; Yu, W.-Y.; Sun, H.-Z.; Liu, W.-S.; Che, C.-M. "Stereo- and enantioselective alkene epoxidations: a comparative study of D4- and D2-symmetric homochiral trans-dioxoruthenium(VI) porphyrins." *Chem. Eur. J.* **2002**, *8*, 2495.
56. Che, C.M.; Zhang, J.-L.; Zhang, R.; Huang, J.-S.; Lai, T.-S.; Tsui, W.-M.; Zhou, X.-G.; Zhou, Z.-Y.; Zhu, N.; Chang, C.K. "Hydrocarbon oxidation by beta-Halogenated dioxoruthenium(VI) porphyrin complexes: Effect of reduction

- potential (RuVI/V) and C-H bond-dissociation energy on rate constants.” *Chem. Eur. J.* **2005**, *11*, 7040.
57. Ho, C.; Leung, W.-H.; Che, C.-M. “Kinetics of carbon-hydrogen bond and alkene oxidation by trans-dioxoruthenium(VI) porphyrins.” *J. Chem. Soc., Dalton Trans.* **1991**, 2933-2939.
58. Zhang, R.; Yu, W.-Y.; Lai, T.-S.; Che, C.-M. “Enantioselective hydroxylation of benzylic C-H bonds by D4-symmetric chiral oxoruthenium porphyrins.” *Chem. Commun.* **1999**, 409.
59. Zhang, R.; Yu, W.-Y.; Lai, T.-S.; Che, C.-M. “Enantioselective epoxidation of trans-disubstituted alkenes by D2-symmetric chiral dioxoruthenium(VI) porphyrins.” *Chem. Commun.* **1999**, 1791.
60. Groves, J.T.; Quinn, R. “Aerobic epoxidation of olefins with ruthenium porphyrin catalysts.” *J. Am. Chem. Soc.* **1985**, *107*, 5790.
61. Groves, J.T.; Bonchio, M.; Carofiglio, T.; Shalyaev, K. “Rapid Catalytic Oxygenation of Hydrocarbons by Ruthenium Pentafluorophenylporphyrin Complexes: Evidence for the Involvement of a Ru(III) Intermediate.” *J. Am. Chem. Soc.* **1996**, *118*, 8961.
62. Gross, Z.; Ini, S. “First Utilization of a Homochiral Ruthenium Porphyrin as Enantioselective Epoxidation Catalyst.” *J. Org. Chem.* **1997**, *62*, 5514.
63. Groves, J.T.; Quinn, R. “Models of oxidized heme proteins. Preparation and characterization of a trans-dioxoruthenium(VI) porphyrin complex.” *Inorg. Chem.* **1984**, *23*, 3844.
64. Leung, W.H.; Che, C.H. “High-valent ruthenium(IV) and -(VI) oxo complexes of

- octaethylporphyrin. Synthesis, spectroscopy, and reactivities.” *J. Am. Chem. Soc.* **1989**, *111*, 8812.
65. Le Maux, P.B.; Bahri, H.; Simonneaux, G. *Chem. Commun.* **1994**, 1287.
66. Le Maux, P.B.; Bahri, H. Simonneaux, G. “Enantioselective Oxidation of Racemic Phosphines with Chiral Oxoruthenium Porphyrins and Crystal Structure of [5,10,15,20-Tetrakis[o-((2-methoxy-2-phenyl-3,3,3-trifluoropropanoyl)amino)phenyl]porphyrinato] ](carbonyl)(tetrahydrofuran) ruthenium(II).” *Inorg. Chem.* **1995**, *34*, 4691.
67. Lai, T.S.; Zhang, R.; Cheung, K.-K.; Che, C.-M.; Kwong, H.-L. “Aerobic enantioselective alkene epoxidation by a chiral trans-dioxo(D4-porphyrinato) ruthenium(VI) complex.” *Chem. Commun.* **1998**, 1583.
68. Suslick, K.S.; Watson, R.A. “Photochemical reduction of nitrate and nitrite by manganese and iron porphyrins.” *Inorg. Chem.* **1991**, *30*, 912.
69. Suslick, K.S.; Watson, R.A. “The photochemistry of chromium, manganese, and iron porphyrin complexes.” *New J. Chem.* **1992**, *16*, 633.
70. Zhang, R.; Newcomb, M. “Laser Flash Photolysis Generation of High-Valent Transition Metal-Oxo Species: Insights from Kinetic Studies in Real Time.” *Acc. Chem. Res.* **2008**, *41*, 468-477.
71. Huang, Y.; Vanover, E.; Zhang, R. “A facile photosynthesis of trans-dioxoruthenium(VI) porphyrins.” *Chem. Commun.* **2010**, *46*, 3776.
72. Gross, Z.; Barzilay, C.M. “A novel facile synthesis of dihalogenoruthenium(IV) porphyrins.” *Chem. Commun.* **1995**, 1287.
73. Zhang, R.; Yu, W.-Y.; Wong, K.-Y.; Che, C.-M. “Highly Efficient Asymmetric



- Epoxidation of Alkenes with a D4-Symmetric Chiral Dichlororuthenium(IV) Porphyrin Catalyst.” *J. Org. Chem.* **2001**, *66*, 8145.
74. Wang, C.; Shalyaev, K.V.; Bonchio, M.; Carofiglio, T.; Groves, J.T. “Fast Catalytic Hydroxylation of Hydrocarbons with Ruthenium Porphyrins.” *Inorg. Chem.* **2006**, *45*, 4769.
75. Vanover, E.; Huang, Y.; Xu, L.; Newcomb, M.; Zhang, R. “Photocatalytic aerobic oxidation by a bis-porphyrin-ruthenium(VI)  $\mu$ -oxo dimer: observation of a putative porphyrin-ruthenium(V)-oxo intermediate.” *Org. Lett.* **2010**, *12*, 2246

## PUBLICATIONS AND PRESENTATIONS

### 1. Peer-Reviewed Journal Publications

1. Zhang, R.\*; Huang, Y.; Abebrese, C.; Thompson, H.; **Vanover, E.**; Webb, C.\*  
“Generation of *trans*-dioxoruthenium(VI) porphyrins: A photochemical approach”  
*Inorg. Chim. Acta*, **2011**, 372, 152-157.
2. Huang, Y.; **Vanover, E.**; and Zhang, R.\* “A facile photosynthesis of *trans*-  
dioxoruthenium (VI) porphyrins”, *Chem. Commun.*, **2010**, 46, 3776-3778.
3. **Vanover, E.**; Huang, Y.; Xu, L.; Newcomb, M.; Zhang, R.\* “Photocatalytic aerobic  
oxidation by a bis-porphyrin-ruthenium(VI)  $\mu$ -oxo dimer: observation of a putative  
porphyrin-ruthenium(V)-oxo intermediate”, *Org. Lett.*, **2010**, 12, 2246-2249.
4. **Vanover, E.**; Lowery, G.; and Zhang, R.\* “Production of Highly Reactive Metal-  
Oxo Species with Molecular Oxygen and Visible Light for the Selective Oxidation  
Catalysis” 2010, *Preprints - American Chemical Society, Division of Petroleum  
Chemistry*, 55 (1).
5. Snyder, Chad A.\*; Tice, Nathan C.; Maddox, Jeremy B.; Emberton, Eric D.;  
**Vanover, Eric S.**; Hinson, Daniel F.; Jackson, Daniel C. “Synthesis, structure, and  
electronic study of some group VII furoyl substituted complexes” *J. Orgmet. Chem.*,  
**2011**, 696(10), 2220-2227.
6. Snyder, Chad A.\*; Tice, Nathan C.; Sriramula, Phenahas G.; Neathery, James L.;  
Mobley, Justin K.; Phillips, Chad L.; Preston, Andrew Z.; Strain, Jacob M.;  
**Vanover, Eric S.**; Starling, Michael P.; et al “Synthesis, characterization, and  
structure of some new substituted 5,6-fused ring pyridazines” *Syn. Comm.*, **2011**,  
41(9), 1357-1369.

## 2 Presentations and Abstracts (presenter)

- 1 Vanover, E. (speaker); Huang, Y.; Abebrese, C.; Webb, C.; Zhang, R.  
Photochemical generation of *trans*-dioxoruthenium(VI) porphyrin complexes, UK  
Naff Symposium 2012, Lexington, KY.
- 2 Vanover, E. (speaker); Huang, Y.; Abebrese, C.; Thompson, T.; Webb, C.; Zhang,  
R. Photochemical generation of *trans*-dioxoruthenium(VI) porphyrin complexes,  
ACS meeting 2012 Spring at San Diego, CA.
- 3 Vanover, E. (speaker); Huang, Y.; Abebrese, C.; Thompson, T.; Webb, C.; Zhang,  
R. Photochemical generation of *trans*-dioxoruthenium(VI) porphyrin complexes,  
2011 KAS annual meeting, Murray, KY
- 4 Vanover, E. (speaker); Zhang, R. A novel photosynthesis of *trans*-  
dioxoruthenium(VI) porphyrin complexes, 2012 WKU Student Research  
Conference, Bowling Green, KY
- 5 Vanover, E.; Huang, Y.; Zhang, R. "Photocatalytic Aerobic Oxidation by a Bis-  
porphyrin-Ruthenium(IV)  $\mu$ -Oxo Dimer through a Putative Porphyrin-  
Ruthenium(V)-Oxo Intermediate" 240th ACS national meeting, Anaheim, CA,  
March 2011.
- 6 Thompson, H.; Abebrese, C.; Huang, Y.; Vanover, E.; Zhang, R. "A novel  
photosynthesis of *trans*-dioxoruthenium(VI) porphyrins", 240th ACS national  
meeting, Anaheim, CA, March 2011.
- 7 Vanover, E.; Huang, Y.; Zhang, R. "Photocatalytic Aerobic Oxidation by a Bis-  
porphyrin-Ruthenium(IV)  $\mu$ -Oxo Dimer" WKU Student Research Conference,  
Bowling Green, KY, March 2011

- 8 Thompson, H.; Abebrese, C.; Vanover, E.; Huang, Y.; Zhang, R. “A novel photosynthesis of *trans*-dioxoruthenium(VI) porphyrins”, WKU Student Research Conference, Bowling Green, KY, March 2011.
- 9 Vanover, E.; Huang, Y.; Zhang, R. “Photocatalytic Aerobic Oxidation by a Bis-porphyrin-Ruthenium(IV)  $\mu$ -Oxo Dimer through a Putative Porphyrin-Ruthenium(V)-Oxo Intermediate”, 96th Kentucky Academy of Science Annual Meeting, Bowling Green, KY, November 2010.
- 10 Vanover, E.; Lowery, G.; Zhang, R. “Production of Highly Reactive Metal-Oxo Species with Molecular Oxygen and Visible Light for the Selective Oxidation Catalysis”, 239th ACS national meeting, San Francisco, CA, March 2010.
- 11 Vanover, E.; Pan, A.; Lowery, G.; Zhang, R. “Kinetics of Oxidation of Aryl Methyl Sulfides by *trans*-Dioxoruthenium(IV) Porphyrin Complexes”, WKU Student Research Conference, Bowling Green, KY, February 2010.
- 12 Vanover, E.; Lowery, G.; Zhang, R. “Photochemical Production of Highly Reactive Metal-Oxo Species for the Selective Oxidation Catalysis”, 95th Kentucky Academy of Science Annual Meeting, Highland Heights, KY, November 2009.
- 13 Vanover, E.; Pan, A.; Lowery, G.; Zhang, R. “Photochemical Production of Highly Reactive Metal-Oxo Species for the Selective Oxidation Catalysis” EPSCoR Annual Meeting, Washington D.C., October 2009.

## ABBREVIATIONS AND SYMBOLS

Ar-H	Aryl hydrogen
$\beta$ -H	Pyrrolic hydrogen
CYP450	Cytochrome P450
CYP450cam	Cytochrome P450cam
DMF	<i>N,N</i> -Dimethylformamide
FID	Flame ionization detector
GC	Gas chromatograph
H <sub>2</sub> (F20-tpp)	5,10,15,20-tetrakis(pentafluorophenyl)porphyrin
<sup>1</sup> H-NMR	Proton nuclear magnetic resonance
H <sub>2</sub> TPFPP	meso-tetrakis(5,10,15,20-pentafluorophenyl)porphyrin
H <sub>2</sub> TPP	<i>meso</i> -tetraphenylporphyrin
KIE	Kinetic isotope effect
$k_0$	Background rate constant
$k_2$	Second-order rate constant
$k_{\text{obs}}$	Observed pseudo-first-order rate constant
<i>m</i> -CPBA	<i>meta</i> -Chloroperoxybenzoic acid
NADH	Nicotinamide adenine dinucleotide
NADPH	Nicotinamide adenine dinucleotide phosphate
PhIO	Iodosylbenzene
[Ru <sup>II</sup> (CO)(4-CF <sub>3</sub> -TPP)]	Carbonyl[4-trifluoromethyl-(5,10,15,20-tetraphenylporphyrinato)] ruthenium(II)
[Ru <sup>II</sup> (CO)TPFPP]	Carbonyl[5,10,15,20-

	tetrakis(pentafluorophenyl)porphyrinato] ruthenium(II)
$[\text{Ru}^{\text{IV}}(4\text{-CF}_3\text{-TPP})(\text{OH})]_2\text{O}$	$\mu$ -oxo-bis[(hydroxo)(4-trifluoromethyl-(5,10,15,20-tetraphenylporphyrinato)) ruthenium(IV)]
$[\text{Ru}^{\text{VI}}(\text{O})_2\text{TPP}]$	<i>trans</i> -dioxo(5,10,15,20-tetraphenylporphyrinato) ruthenium(VI)
$[\text{Ru}^{\text{VI}}(\text{O})_2\text{TPFPP}]$	<i>trans</i> -dioxo[5,10,15,20-tetraphenylporphyrinato] ruthenium(VI)
TBHP	<i>tert</i> -Butyl hydroperoxide
TONs	Turnover numbers
UV-vis	Ultraviolet-visible

